

NASA/TM-2013-218024



# Analysis Methods for Progressive Damage of Composite Structures

*Cheryl A. Rose, Carlos G. Dávila, and Frank A. Leone  
Langley Research Center, Hampton, Virginia*

July 2013

## NASA STI Program . . . in Profile

Since its founding, NASA has been dedicated to the advancement of aeronautics and space science. The NASA scientific and technical information (STI) program plays a key part in helping NASA maintain this important role.

The NASA STI program operates under the auspices of the Agency Chief Information Officer. It collects, organizes, provides for archiving, and disseminates NASA's STI. The NASA STI program provides access to the NASA Aeronautics and Space Database and its public interface, the NASA Technical Report Server, thus providing one of the largest collections of aeronautical and space science STI in the world. Results are published in both non-NASA channels and by NASA in the NASA STI Report Series, which includes the following report types:

- **TECHNICAL PUBLICATION.** Reports of completed research or a major significant phase of research that present the results of NASA Programs and include extensive data or theoretical analysis. Includes compilations of significant scientific and technical data and information deemed to be of continuing reference value. NASA counterpart of peer-reviewed formal professional papers, but having less stringent limitations on manuscript length and extent of graphic presentations.
- **TECHNICAL MEMORANDUM.** Scientific and technical findings that are preliminary or of specialized interest, e.g., quick release reports, working papers, and bibliographies that contain minimal annotation. Does not contain extensive analysis.
- **CONTRACTOR REPORT.** Scientific and technical findings by NASA-sponsored contractors and grantees.

- **CONFERENCE PUBLICATION.** Collected papers from scientific and technical conferences, symposia, seminars, or other meetings sponsored or co-sponsored by NASA.
- **SPECIAL PUBLICATION.** Scientific, technical, or historical information from NASA programs, projects, and missions, often concerned with subjects having substantial public interest.
- **TECHNICAL TRANSLATION.** English-language translations of foreign scientific and technical material pertinent to NASA's mission.

Specialized services also include organizing and publishing research results, distributing specialized research announcements and feeds, providing information desk and personal search support, and enabling data exchange services.

For more information about the NASA STI program, see the following:

- Access the NASA STI program home page at <http://www.sti.nasa.gov>
- E-mail your question to [help@sti.nasa.gov](mailto:help@sti.nasa.gov)
- Fax your question to the NASA STI Information Desk at 443-757-5803
- Phone the NASA STI Information Desk at 443-757-5802
- Write to:  
STI Information Desk  
NASA Center for AeroSpace Information  
7115 Standard Drive  
Hanover, MD 21076-1320

NASA/TM-2013-218024



# Analysis Methods for Progressive Damage of Composite Structures

*Cheryl A. Rose, Carlos G. Dávila, and Frank A. Leone  
Langley Research Center, Hampton, Virginia*

National Aeronautics and  
Space Administration

Langley Research Center  
Hampton, Virginia 23681-2199

---

July 2013

The use of trademarks or names of manufacturers in this report is for accurate reporting and does not constitute an official endorsement, either expressed or implied, of such products or manufacturers by the National Aeronautics and Space Administration.

Available from:

NASA Center for AeroSpace Information  
7115 Standard Drive  
Hanover, MD 21076-1320  
443-757-5802

## Contents

1	Introduction	2
2	Modeling Multiple Damage Mechanisms and their Interactions	1
2.1	Cohesive Models for Fracture in Composite Structures	4
2.1.1	Modeling Delamination Propagation in the Presence of Fiber Bridging	5
2.1.2	Improved Cohesive Models for Mixed-Mode Fracture	6
2.1.3	Cohesive Laws for Adhesive Modeling	7
2.1.4	Cohesive Elements for Improved Computational Efficiency	8
2.1.5	Extensions Required for Fatigue Loading	8
2.1.6	Summary, Cohesive Models for Fracture in Composite Structures	8
2.2	Continuum Damage Mechanics Models	9
2.2.1	Material Property Characterization	10
2.2.2	Limitations of Continuum Damage Mechanics Models	15
2.2.3	Refinements to CDM Models	18
2.2.4	Summary, Continuum Damage Mechanics Models	20
2.3	Discrete Damage Modeling Methods	21
2.3.1	Mesh Sensitivity/Refined Cohesive Elements for Proper Interaction	23
2.3.2	Crack Initiation, Saturation and Delamination Onset	24
2.3.3	Extensions for Compression after Impact and Fatigue Loading	25
2.3.4	Summary, Discrete Damage Models	25
3	Experimental Methods	26
3.1	Measuring Initial Imperfections with Coordinate Measurement Machine	27
3.2	Ultrasonic Inspection	28
3.3	Digital Image Correlation	29
3.4	X-Ray Computed Tomography	30
3.5	Summary, Experimental Methods	31
4	Applications	32
4.1	Damage Tolerance of Post Buckled Stiffened Panels	32
4.2	Open-Hole Tension	34
5	Summary	37

## 1 Introduction

This document provides an overview of recent accomplishments and lessons learned in the development of general progressive damage analysis methods for predicting the residual strength and life of composite structures. The developments described were accomplished by the authors and university collaborators while supporting the Subsonic Rotary Wing (SRW) Project, the Aircraft Aging and Durability (AAD) Project and the Vehicle Systems Safety Technologies (VSST) project. These developments are described within their State-of-the-Art (SoA) context and the associated technology barriers. The emphasis of the authors is on developing these analysis tools for application at the structural level. Hence, modeling of damage progression is undertaken at the mesoscale, where the plies of a laminate are represented as a homogenous orthotropic continuum.

There are several primary motivations for developing analysis methods to model onset and growth of damage in composites. One is to eliminate some of the testing requirements in the building block approach used for design and certification of composite primary structures. By replacing the tests of subcomponents and components normally performed during the intermediate stages of the building block process, significant savings can be realized in terms of costs and the time required to progress from preliminary design to service. The second motivation for developing these analyses is to enable parametric studies to assess the relative severity of possible damage modes in new design concepts. Such a predictive capability offers the potential for the development of more efficient concepts by enabling the exploration of the large design space of laminated composites, which is not possible with the current largely empirical approach for structural design and substantiation. An additional motivation is to provide tools for assessing the safety of as-built structures and the structural integrity in the presence of manufacturing imperfections or flaws and in-service damage.

To predict reliably composite structural residual strength and life, general purpose progressive analysis tools capable of representing all of the composite damage modes (matrix cracking, delamination, fiber kinking, fiber breakage, etc.) and their interactions are needed. Of particular relevance for structural applications is the development of an improved understanding of the significance of interactions between matrix cracking and delaminations on structural life and strength, and the development of analysis methods to represent these interactions. For instance, correct representations of the effects of matrix cracks and delamination on fiber kinking failure phenomena are essential for accurate prediction of compression after impact strength. In addition, several studies have demonstrated that matrix shear nonlinearity can influence these interactions, and must be included in simulations. Due to the complexity of the failure processes that must be captured by the predictive models, the implementation of these capabilities into robust and accurate analysis software can only be achieved in incremental steps.

The following sections provide a brief examination of the major advances in the SoA of progressive damage analysis for composite structures. The aim of the present effort is to establish the ranges of validity of available models, to identify technology barriers, and to establish the foundations of the future investigation efforts. Such are the necessary steps towards accurate and robust simulations that can replace some of the expensive and time-consuming “building block” tests that are currently required for the design and certification of aerospace structures.

## 2 Modeling Multiple Damage Mechanisms and their Interactions

Modeling progressive failure in composite materials and structures remains a challenge after years of extensive research due to the large number of damage mechanisms that must be considered and their complex interactions. Fracture in a composite structure is the result of the evolution and interactions of discrete damage events such as fiber/matrix debonding, matrix cracking, delamination between plies, and fiber failure. Additionally, the effect of shear deformation on crack onset has been observed experimentally [1] and analyses have found that such nonlinearities must be represented by the models for an accurate prediction of the evolution of interacting matrix and delamination cracks [2-4]. These damage modes evolve in various combinations that depend on the laminate geometry and stacking sequence and cause redistributions of stresses in the failing composite. Some combinations of damage may reduce local stress concentrations, while others may precipitate a structural collapse. Therefore, an analysis methodology capable of predicting structural strength and fatigue life must take into account damage initiation and propagation.

However, the details of the mechanisms that lead to failure are not fully understood due to the complexity involved with the idealization of the individual constituent responses and their interactions. The presence of two constituents, fiber and matrix, and the extreme anisotropy in both stiffness and strength properties result in damage mechanisms that act at different scales. The damage mechanisms can be divided into intralaminar and interlaminar damage. As shown in Fig. 1, intralaminar damage mechanisms correspond to fiber fracture and matrix cracking, whereas interlaminar damage mechanisms correspond to the interfacial separation of the plies (delamination).

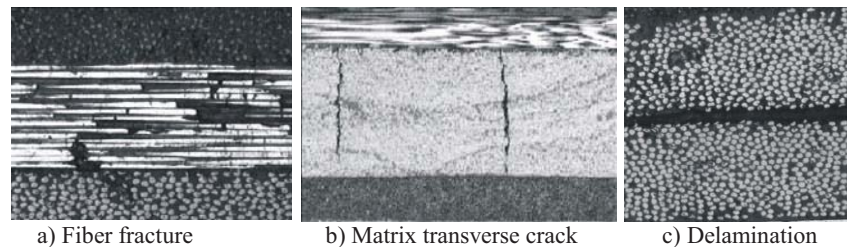


Fig. 1. Damage mechanisms in laminated composites.

The formulation of the governing physical principles of damage evolution depends on the scale of the idealization of the damage process, which may span from molecular dynamics to structural mechanics, and includes the intermediate scales of micro- and meso-mechanics. The damage models shown in Fig. 2 illustrate four typical scales of damage idealization. The micromechanical model shown in Fig. 2a represents what is normally the lowest practical scale of composite damage idealization, in which detailed matrix damage mechanisms, such as matrix plasticity and cracking, as well as fiber/matrix interface cracking are typically represented using representative volume element (RVE) [5], or unit cell models. The representation of damage at this level is typically based on a reduction of the material stiffness. Hence, fracture is represented as a band of localized volumetric stiffness reduction, referred-to as “soft discontinuity” as opposed to a “hard discontinuity” where voids are represented by displacement discontinuities in the model. Due to computational constraints, micromechanical models are typically two-dimensional and they represent domains much smaller than a ply thickness. Consequently, they are useful for representing a composite hardening response, before cracks localize at the ply level or larger scale.

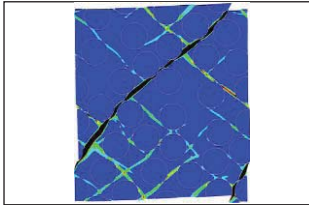
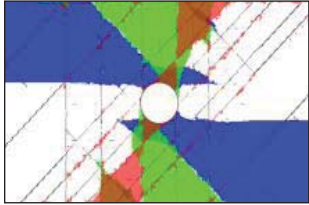
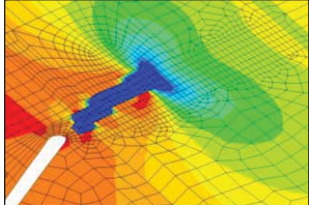
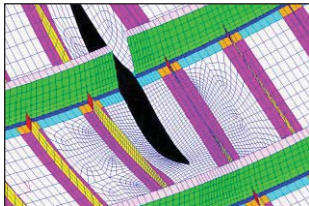
	<b>Scale of idealization</b>	<b>Damage type</b>	<b>Typical approaches</b>
	<b>a. Micromechanical (Soft discontinuity)</b>	Fiber/matrix interface, matrix plasticity and damage	<ul style="list-style-type: none"> <li>• RVE models (unit cell)</li> </ul>
	<b>b. Mesoscale (Hard discontinuity)</b>	Discrete damage	<ul style="list-style-type: none"> <li>• xFEM + Cohesive laws</li> </ul>
	<b>c. Mesoscale (Soft discontinuity)</b>	Intralaminar damage	<ul style="list-style-type: none"> <li>• Continuum damage models (CDM)</li> </ul>
	<b>d. Structural (Hard discontinuity)</b>	Through-the-thickness crack or delamination	<ul style="list-style-type: none"> <li>• Fracture mechanics and modifications</li> <li>• Strain softening, cohesive laws</li> </ul>

Fig. 2. Levels of damage idealization, from micromechanical to structural.

The most common idealizations of composite damage for representing structural level response are at the mesoscale level, where the individual plies are represented as homogenous, anisotropic materials (Fig. 2b and Fig. 2c). At this level, the intralaminar and interlaminar damages processes have traditionally been treated using different theories. Intra-ply damage modes have been investigated primarily within the framework of Continuum Damage Mechanics (CDM) [6], where damage modes are represented as a reduction in the corresponding stiffnesses. Delamination has been studied extensively using interface fracture modeling techniques such as cohesive zone models [7] and virtual crack closure techniques (VCCT) [8, 9]. Direct coupling of the intralaminar damage models with the interlaminar damage models is accomplished by incorporating both damage models within a single finite element model. Despite significant advances in progressive damage modeling, recent studies [10, 11] have indicated that CDM models for ply failure, coupled with cohesive zone models for delamination have difficulty in accurately representing laminate failure sequences that are characterized by strong coupling between matrix cracking and delamination. Among the limitations of the CDM models that contribute to this difficulty, are their inability to accurately predict matrix crack paths, and to describe accurately local effects of stress redistribution in a damaged area.

To address the limitations in the CDM framework, recent emphasis has been placed on development of discrete damage models (DDM) at the meso-scale level with discrete representation of cracks of all types, so that their coupling can be directly accounted for in a prediction. Progress in this area has been enabled by nonlinear cohesive zone models of fracture, and critical developments in computational finite elements, based upon the eXtended Finite



Element Method (X-FEM), that allow arbitrary cracks to initiate and propagate within a simulation, independently of the finite element mesh.

Finally, the model of a through-crack in a fuselage panel shown in Fig. 2d illustrates an example of a structural-level damage model. The crack is represented as a hard discontinuity, and prediction of the propagation of the crack could be based on a strain-softening law or a criterion based on the critical energy release rate [12]. However, any structural-level crack propagation criterion is strongly dependent on the material system and laminate configuration and, consequently, must be determined for each new material system and laminate stacking sequence. In addition, structural-level semi-empirical fracture models cannot address the characteristics of the crack-tip damage zone nor the complex interactions between micro- and macro-failures associated with the crack-extension process. Instead, the crack-tip damage zone is simulated as some “effective” notch-tip damage zone that is assumed to grow in a self-similar manner. In many cases, self-similar crack growth is not observed, and the lack of resolution in the damage mechanisms often renders structural-level models inaccurate after a short propagation of damage.

It is clear from the preceding overview of typical damage modeling strategies that the conceptual idealization of damage, i.e., the identification, characterization, and formulation of the governing physical mechanisms that constitute damage evolution, are different at each scale of idealization. Damage idealizations with higher resolution and kinematic freedom can capture multiple damage mechanisms with a separate damage law for each mechanism. These damage laws are likely to be simpler and require a fracture toughness that is lower than required in the damage laws used in coarser models to represent the same global response. For instance, meso-scale discrete-damage models may only need one simple cohesive law to represent a variety of matrix damage patterns, while CDM models need multiple empirical stiffness degradation laws and interacting activation functions to represent the softening of the material.

Two computational schemes are being pursued for developing the analysis capability required for predicting strength and life of composite structures. In one approach, a CDM model for in-plane damage is coupled with cohesive elements for interface damage. The second approach employs a DDM method for matrix cracking, in combination with cohesive elements for delamination. A critical distinction between the CDM methodology and DDM interface fracture models exists in the approach in which a displacement discontinuity is represented; i.e. the CDM methodology replaces the displacement discontinuity with local volumetric stiffness degradation, or a “soft discontinuity,” whereas the interface fracture based techniques directly include the kinematics of the displacement jump. The “soft discontinuity” approach used in the CDM models leads to some limitations of the CDM models, as described above. However, there are significant advantages of the CDM methodology which include relative maturity, general formulations and implementations in commercial finite element codes, the ability to describe in a computationally tractable manor the stiffness response of a laminate with large amounts of matrix damage, and the ability to represent all failure modes, including the onset and evolution of fiber failure which does not follow a predefined path.

Recent applications of the DDM models [2, 4, 13, 14] have demonstrated high fidelity in their predictions for situations in which CDM approaches are limited, specifically failure scenarios dominated by matrix and delamination cracking. However, demonstrations to date have been for monotonic tension loading only; extension and validation for other loading cases requires extensive testing. Additionally, the developments for composite structures where multiple cracks in individual layers interact with each other, with multiple cracks in adjacent layers, and with delaminations between layers, are relatively immature. Furthermore, typical implementations are two-dimensional and do not include bending deformations, implementations in finite commercial finite element codes are limited, and extensions required to include interactions with fiber failure are not clear. Finally, the fine meshes required for representing the nonlinear fracture process zones of multiple cracks and their interactions may render these models intractable for simulations beyond the coupon level.

The remainder of the document is organized as follows. First, cohesive laws for representing nonlinear fracture processes are briefly described. These cohesive laws are used in the formulations of the cohesive elements for interface fracture, and for predicting the initiation and propagation of matrix cracks in the DDM models. In the DDM models, the same cohesive laws are used for matrix and delamination cracking. Recent advancements in determining complex cohesive laws for fracture processes where multiple energy dissipating mechanisms contribute to crack growth resistance are described, along with limitations for predicting crack growth under mixed-mode crack conditions. Extensions required for addressing fatigue loading, and for incorporating compression loading are also described. Then, the concepts of the continuum representation of composite material response are discussed and the intrinsic limitations of CDM models for laminated composites are outlined. A summary of recent developments to address these limitations and developments in experimental methods for determining critical material property input are presented as well. Next, an emerging DDM modeling technique based on the eXtended Finite Element Method (X-FEM) that overcomes many of the limitations of CDM models is presented. Capabilities of the CDM and DDM modeling techniques are then illustrated with some examples. Finally, advancements in experimental methods that have contributed to the validation of the methods are described, along with some suggestions for future required developments. To address the overall objective of the document, each section closes with a bulleted summary of the SoA, recent developments, and known technology barriers relevant to that section.

## 2.1 Cohesive Models for Fracture in Composite Structures

The ability to predict crack propagation in composites emerged four decades ago with the development of computational methods based on the theory of linear elastic fracture mechanics (LEFM). However, LEFM is limited to applications in which the fracture process zone is confined to the immediate neighborhood of the crack tip itself, or the fracture process zone is small compared to the characteristic crack length. For many fracture processes in composite materials and structures, the fracture process zone may be relatively large compared to other structural dimensions. The fracture process zone is a nonlinear zone characterized by plastic deformations and progressive material softening due to nonlinear material deformations, such as microcracking, void formation and fiber/matrix pullout. The size of the fracture process zone is dependent on the type of material softening and it must be considered in many situations of crack growth in composite structures. For example, development of a process zone gives rise to stable growth and crack growth resistance. The apparent fracture toughness increases with crack growth – an effect called the *R-curve* – until the process zone is fully developed.

Nonlinear fracture mechanics (NLFM) provides a framework for characterizing crack growth resistance and for analyzing initial amounts of stable crack growth. The cohesive zone model is a NLFM methodology that was developed to simulate the nonlinear fracture response near the crack tip, by collapsing the effect of the nonlinear process zone onto a surface of displacement discontinuity. Additionally, cohesive crack models have the ability to describe the process of void nucleation from inclusions. Therefore, they can be applied to initially un-cracked structures and can describe the entire fracture process, from no crack to complete structural failure.

Cohesive crack models are based on kinematic descriptions that use discontinuities in the displacement field. Cohesive interfacial laws are phenomenological mechanical relations between the tractions and interfacial separations such that, with increasing interfacial separation, the tractions across the interface reach a maximum, and then decrease and vanish when complete decohesion occurs. It can be shown by performing a J-integral calculation along a contour surrounding a notch tip that the resulting work of interfacial separation is related to Griffith's fracture criterion [15]:

$$G_c = \int_0^{\delta_f} \sigma(\delta) d\delta \quad (1)$$

where  $G_c$  is the critical energy release rate, and  $\sigma$  and  $\delta$  are the interfacial traction and interfacial separation, respectively.

Cohesive zone models have been used extensively in composite fracture analysis to represent multiple cohesive mechanisms acting across delamination or other types of cracks. For many common fracture processes in composite materials and structures, the apparent fracture toughness increases with crack growth. Such a response is typically due to the presence of more than one physical phenomenon involved in the separation process: some acting at small opening displacements, which are confined to correspondingly small distances from the crack tip, and others acting at higher displacements and extending further into the crack wake. In the presence of an *R-curve*, the toughness measured during crack propagation typically increases monotonically until reaching a steady-state value. In the case of delamination, the increase in toughness with crack growth is attributed to fiber bridging across the delamination plane.

### 2.1.1 Modeling Delamination Propagation in the Presence of Fiber Bridging

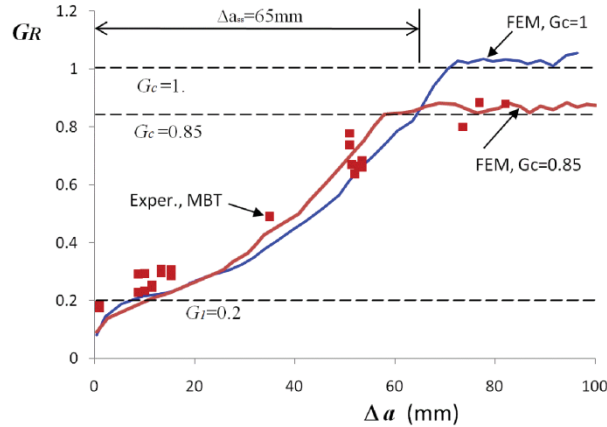


Fig. 3. R-curves for DCB specimen obtained by cohesive element superposition.

The interlaminar crack growth resistance of long fiber-reinforced composites can significantly increase in the presence of fiber bridging, which induces tractions that act over an extended zone in the wake of the crack tip. As a consequence, the *R-curve* of unidirectional composites in Mode I delamination is characterized by a fracture toughness that gradually increases from an initial value of  $G_I$  up to a value corresponding to steady-state propagation,  $G_c$  [16, 17], as shown in Fig. 3. To avoid the difficulties associated with *R-curve* effects, standard test methods such as ASTM D5528 [18] conservatively recommend the use of fracture initiation values to characterize the toughness of double cantilever beam (DCB) specimens. However, the use of the energy release rate measured at the initiation of nonlinearity causes a severe underestimation of the predicted strength, regardless of whether linear elastic fracture mechanics or cohesive zone models are used. Conversely, the use of the critical energy release rate for steady state propagation leads to a severe overestimation of the strength [16]. Therefore, for accurate predictions of strength, it is necessary to have a model that accounts for the *R-curve* effect.

The complex fracture processes involved in the delamination of composites can be approximated by superposing two or more different cohesive laws. The use of linear and non-linear cohesive laws to model fiber bridging in delamination has been explored by many authors. It has been shown that softening laws within cohesive elements can be used to represent bridging as well as the dominant fracture process. The superposition of two bilinear cohesive responses was applied to model fiber bridging in the tensile fracture of unidirectional composites in Dávila et al. [16]. The trilinear cohesive law that results has also been used as an approximation of the complex fracture processes involved in the delamination of composites [19-22]. The principal difficulty in the use of superposed cohesive laws to represent *R*-curve effects is the lack of validated methodologies for the calibration of the softening laws. In addition, the development of a procedure for material parameter identification from DCB test results is complicated by several factors. It is known that the *R*-curves obtained are dependent on the specimen geometry and that there are no direct procedures for extracting bridging laws from experimental *R*-curves. Finally, the extraction of energy release rate (ERR) using standard procedures may be inaccurate for problems with large-scale bridging.

In a recent study [23], experimental measurements were conducted to determine the critical ERR of glass/epoxy and its associated *R*-curve effect using DCB specimens. Then, the use of trilinear cohesive laws obtained by the superposition of simpler bilinear cohesive laws for representing the *R*-curve was investigated. Two approaches for determining the parameters of the superposed cohesive laws were proposed. In the first approach a procedure for extracting the cohesive parameters from experimental *R*-curves through the use of a new semi-analytical equation was developed. The methodology was applied to the experimental DCB data and it was shown that the resulting model was able to reproduce well the force-displacement response as well as the desired *R*-curve. In the second approach, an experimental *R*-curve is not required, and the parameters were obtained using a numerical optimization procedure that reduces the error between the predicted and experimental force-displacement results. The second approach is advantageous when fiber bridging introduces inaccuracies in the experimental energy release rate measurements. In addition, the second approach can be extended to identify the parameters needed for using more complex approximations of the cohesive laws.

### 2.1.2 Improved Cohesive Models for Mixed-Mode Fracture

In structural applications of composites, crack growth is likely to occur under mixed-mode loading. The loads and the number of cycles necessary to propagate constrained cracks such as delaminations are strongly dependent on the mode mixity, i.e. the ratio of the opening and shearing energies used in the formation of a new crack surface. Therefore a general formulation of cohesive laws must address mixed-mode fracture. Despite the maturity of cohesive laws, some issues regarding the prediction of crack propagation under mixed-mode conditions remain unresolved. It has recently been observed that although the global fracture mode mixity is constant throughout loading, the local fracture mode mixity is almost never constant during the damage evolution. Experiments by Högberg et al. [24] and analyses using cohesive elements show that the instantaneous mode mixity changes during the process of damage. It was found that damage initiation is usually dominated by transverse shear (Mode II) and, as damage evolves, the fracture process becomes increasingly dominated by Mode I opening. Consequently, the history of the interfacial traction,  $\tau^o$ , versus displacement,  $\Delta^f$ , relationship is not bilinear, as intended, but rather transitions from one bilinear function to the next, resulting in a concave curve as shown in red in Fig. 4. Unfortunately, all cohesive formulations assume that the mode mixity is constant during damage evolution. Therefore, cohesive and fracture models may not predict the correct propagation of fracture.

In specimens such as the Mixed Mode Bending (MMB) specimen or the Double Cantilever Beam specimen with Uneven Bending Moments (DCB-UBM), where the fracture mode mixity

from a linear elastic viewpoint is independent of crack length, it is observed that all points along the crack path undergo the same history of mode change during damage.

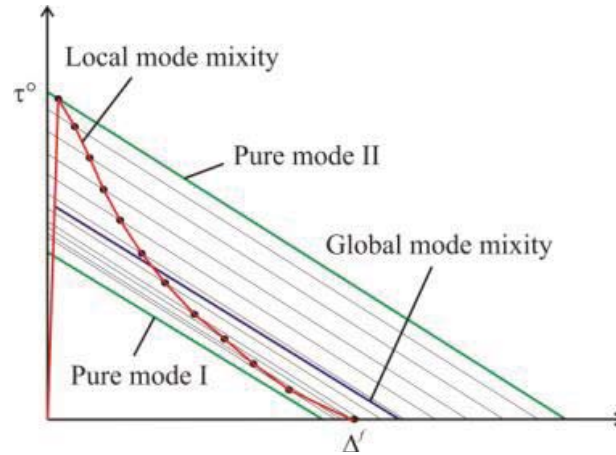


Fig. 4. Predicted instantaneous and global traction displacement laws in local mixed mode.

An investigation is ongoing to understand better the significance of the dependence of the fracture propagation on the history of the mode mixity. The initial approach to this investigation consisted in a mathematical evaluation of the conditions under which cohesive element formulations are thermodynamically consistent. It was found that by imposing the so-called “Turon Constraint” [25, 26] a mixed-mode cohesive model can be derived from an energetic potential, therefore satisfying the laws of damage irreversibility and energy dissipation. However, such a model does not always tend to the linear elastic solution, even in cases of short process zones, as initially expected. It was also found that mixed-mode cohesive laws can reproduce exactly the analytical results only in specific cases which result in path independence. Additional work is needed to understand which results are correct and what cohesive models ensure that crack propagation is correctly predicted for all loading conditions and materials.

### 2.1.3 Cohesive Laws for Adhesive Modeling

A methodology using Digital Image Correlation (DIC) was developed to characterize the mixed-mode fracture properties of composite joints bonded with Cytec FM-300M mat-reinforced structural adhesive [27]. A test campaign was conducted using three types of specimens. Double Cantilever Beam (DCB), End Notch Flexure (ENF) and Mixed-Mode Bending (MMB) tests were performed on carbon-epoxy specimens to determine the Mode I, Mode II, and mixed-mode fracture properties, respectively.

The characterization procedure uses DIC to extract the displacement histories around the initial crack tip, including the rigid body rotations as well as the shearing and opening displacement jumps across the crack tip. Following an inverse methodology, these displacement jumps are substituted into analytical J-integral equations that describe the fracture energy in terms of the rotations and displacement jumps at the crack tip. Finally, the cohesive laws needed for finite element analysis are obtained by numerical differentiation of the J-integral functions. The resulting cohesive laws represent the adhesive stiffness, its strength, and its fracture resistance in the form of stress-displacement functions in each mode of fracture.

The prediction of mixed-mode fracture of adhesives is particularly challenging because it is difficult to satisfy the “Turon Constraint” [26] that ensures the correct energy dissipation. It was



found that without the imposition of this constraint, that the mode mixity is improperly computed by the elements and the predicted results are inaccurate. Additional research is necessary to develop a mixed-mode cohesive model that is not restricted by the assumptions of the Turon model.

The measured cohesive laws were approximated using piecewise linear functions for numerical implementation into User defined cohesive ELements (UEL). The results from the numerical simulations of the test specimens confirm that the measured cohesive laws in combination with the UEL can be used to predict the debonding process in mixed mode, including the initiation of damage as well as steady-state tearing.

#### 2.1.4 Cohesive Elements for Improved Computational Efficiency

One of the major drawbacks of cohesive elements is their requirement for fine meshes. Recent investigations have attempted to quantify a priori the mesh requirements and to establish procedures to determine the parameters that describe the cohesive laws. However, many structural problems remain computationally intractable due to these mesh requirements. Research is needed to identify solutions to reduce these mesh requirements. The solutions might require hybrid cohesive/VCCT formulations, and/or cohesive elements with advanced integration schemes.

#### 2.1.5 Extensions Required for Fatigue Loading

Delamination can occur due to the accumulation of damage under both static and cyclic loads. Constitutive models for decohesion must be able to describe both types of material degradation. Models that extend the cohesive zone modeling approach for monotonic loading into forms suitable for cyclic loading, such as Turon [28], have not yet been thoroughly validated. In addition, very few models have been proposed that are truly predictive, i.e., that depend on measurable properties such as the Paris Law coefficients rather than relying on parameter calibrations that may be dependent on mesh refinement, mode mixity, R-ratio,  $G_{max}$ , etc. Much work is needed to characterize experimentally the phenomena that lead to fatigue crack propagation, and to develop phenomenological laws that capture these effects.

Finally, cohesive models always require fine meshes. However, in the case of fatigue loading, the mesh requirements quickly become intractable. Additional work is needed to reduce the requirements to have such excessively refined meshes. As in the case of quasi-static analyses, solutions that would alleviate the mesh requirements include hybrid cohesive/VCCT formulations, and cohesive elements with advanced integration schemes.

#### 2.1.6 Summary, Cohesive Models for Fracture in Composite Structures

##### **2.1 Cohesive Models for Fracture in Composite Structures**

###### ***State of the Art***

- *Cohesive element technology has good degree of maturity as a robust prediction tool. Cohesive elements are becoming available in most commercial FEM software suites.*

###### ***Recent Advances***

- *Procedures have been developed to determine a priori the parameters that describe the cohesive laws and the maximum size of the finite elements needed for proper energy dissipation.*

- *Relationships between the shape of a cohesive law and the R-curve effects are better understood.*
- *Progress made towards thermodynamically-consistent cohesive law formulation: definition of “Turon Constraint.”*
- *Measurement of cohesive laws for adhesive failure in mode I and mode II demonstrated.*

#### **Technology Barriers**

- *Mixed-mode fracture poses challenges that are not well understood. Issues of path dependence must be addressed.*
- *Fatigue cohesive formulations are immature.*
- *Fatigue cohesive models have mesh requirements that are intractable.*

#### **LaRC Cohesive Element Research Software**

- *Coh\_UEL.03 (LaRC, [7])*
  - *8-node cohesive element with 3 DOF/node based on LaRC B-K criterion for mixed-mode fracture.*
  - *Secant stiffness only.*
  - *User-written UEL subroutine for Abaqus/Std.*
- *Coh\_UEL.06 (LaRC, Turon, U. of Girona, [29])*
  - *Thermodynamically-consistent constitutive model.*
  - *Analytically-derived tangent stiffness.*
- *Coh\_UEL\_Fatigue.06 (Turon, U. of Girona, [28])*
  - *Fatigue damage model based on Turon’s PhD dissertation.*
- *Coh\_UEL\_Shell.07 (LaRC, [30]).*
  - *8-node cohesive element with 6 DOF/node allows connection of shell elements without requiring coincident nodes.*
- *Coh\_UEL.12 (Sarrado/Turon U. of Girona, [26])*
  - *Numerical tangent stiffness for ease of constitutive model development and improved convergence rate.*
  - *Interlaminar shear stiffness is calculated internally for thermodynamic consistency in mixed-mode.*

## **2.2 Continuum Damage Mechanics Models**

The most common idealizations for representing the initiation and evolution of intralaminar damage modes in structural level predictions rely on meso-scale level continuum damage mechanics (CDM) models. At the meso-scale level, individual plies of a laminate are assumed to be composed of a homogeneous material with orthotropic properties. Continuum damage mechanics models for composite materials were pioneered by Ladevèze, Matzenmiller [31, 32] and others based on previous work by Kachanov, Lemaître [33, 34] and others. In-house analysis efforts have used primarily the Progressive Damage Model for Composites provided in Abaqus

[35] and the continuum damage model originally proposed by Maimí [36]. In these composite damage models, a distinction is made between the different failure modes, especially between fiber and matrix failure, and damage is represented by progressively degrading appropriate stiffnesses in accordance with predefined failure criteria. There are many failure criteria that have been proposed to predict the onset of matrix cracking and fiber fracture, some of which are described and compared in the World Wide Failure Exercise [37, 38]. However, few criteria can represent several relevant aspects of the failure process of laminated composites, e.g. the increase of apparent shear strength when applying moderate values of transverse compression, or the detrimental effect of the in-plane shear stresses in failure by fiber kinking. The LaRC03 failure criteria [39] and subsequent evolutions [40] address some of the limitations of other failure criteria as identified from the WWFE. For example, the LaRC criteria account for the effect of ply thickness, fiber misalignment in compression, and the effect of shear nonlinearity on fiber kinking and in-situ strength.

In the model proposed by Maimí [36], the LaRC04 failure criteria [40] are used as damage activation functions,  $F_M$ , to formulate a continuum damage model to predict the propagation of the several ( $M$ ) damage mechanisms occurring at the intralaminar level. Each damage activation function predicts one type of damage mechanism using the following equations:

$$F_M := \phi_M(\sigma^t) - r_M^t \leq 0 \quad (2)$$

where  $r_M^t$  are internal variables (equal to 1 at time  $t = 0$ ), and the functions  $\phi_M(\sigma^t)$  correspond to the LaRC04 failure criteria. When a damage activation function is satisfied,  $F_M = 0$ , the associated damage variable,  $d_M$ , is greater than zero, and the ply compliance tensor is affected by the presence of damage. Once a damage initiation criterion is satisfied further loading causes reduction of the material stiffness coefficients. The reduction of the stiffness coefficients is controlled by the damage variables, whose evolutions in the post-damage initiation phase are represented by softening laws.

In many damage models, including the Progressive Damage Model for Composites provided in Abaqus [35] and most cohesive laws, the evolution of damage is represented with bilinear laws that are described by a maximum traction and a critical energy release rate. The computational implementation of softening constitutive equations poses difficulties, however, because the boundary value problem becomes ill-posed when strain localizes along a surface known as the failure surface, leading to mesh subjective schemes [41]. Upon reducing the element sizes to zero, these analysis models predict failure to occur with zero energy dissipation. To resolve this lack of objectivity with respect to element size, a characteristic length is introduced into the constitutive model using a procedure based on the crack band model proposed by Bažant and Oh [42]. A complete definition of a continuum damage model for the simulation of intralaminar damage can be found in [43].

### 2.2.1 Material Property Characterization

The Abaqus damage model and the damage model described in the 2006 NASA TM [36] use as input ply-level material properties and fracture toughness values. The use of ply-level properties is advantageous because standard test methods are available for determining the majority of the material properties required for input to the damage model, imperfections and variabilities that must be considered at lower scales can be disregarded, and use of ply-level properties eliminates testing requirements to determine material property input for the damage models every time the lay-up or stacking sequence is changed. These models require as input the material properties below:



- Ply elastic properties ( $E_1, E_2, G_{12}, G_{23}, \nu_{12}, \nu_{23}$ ) and ply strengths ( $X_T, X_C, Y_C, S_L$ ).
- Four components of the fracture toughness associated with longitudinal failure in tension and compression ( $G_{I+}$  and  $G_{I-}$ , respectively) and transverse cracking in mode I and II, ( $G_{2+}$  and  $G_6$ , respectively)

All of the ply elastic and strength properties, with the exception of the ply shear strength, can be determined using test standards defined by the American Society for Testing Materials (ASTM). Traditionally, due to limited characterization data, it has been assumed that predictions of the growth of intralaminar cracks can be based on the fracture toughness values for growth of interlaminar cracks. The mode I fracture toughness component for transverse matrix cracking,  $G_{2+}$ , is therefore determined using the Double Cantilever Beam (DCB) test ASTM-D 5528, and  $G_6$  can be determined using the four-point bending end-notched flexure test [44]. Recent experimental studies to determine mode I intralaminar fracture toughness from compact tension tests have confirmed that the intralaminar and interlaminar mode I fracture toughness values are equal [45].

***Resistance Curves in Fiber Failure of Composites.*** There are no standard test methods for determining the fracture toughness associated with longitudinal failure in tension and compression. It has been recommended that the fracture toughness for tensile longitudinal failure be determined using the compact tension test developed by Pinho [46]. Recently a new methodology was proposed to measure the crack growth resistance curves (*R*-curves) associated with fiber-dominated failure modes directly from these tests. The proposed methodology is based on identification of the crack tip location using the Digital Image Correlation (DIC) technique and the calculation of the J-integral directly from the test data using a simple closed form expression derived explicitly for the specimen lamination sequence [47]. The method obviates the need of any complex pre- and post-processing of the test data, either based on finite element calculations or standard data reduction methods, and enables the real-time generation of *R*-curves during a test.

The crack-growth resistance curves obtained not only characterize the fracture toughness of the material, but they also provide the basis for identification of the parameters of the softening laws used in the numerical simulation of the longitudinal fracture in the continuum damage mechanics models. The shape of the softening law is often assumed to be inconsequential for prediction of fracture, provided that it is defined as a function of the fracture toughness. While this assumption is valid when crack propagation is governed primarily by a single energy dissipating mechanism, the shape of the cohesive law plays a critical role in the prediction of fracture when crack propagation includes multiple energy dissipation mechanisms that act over different length scales. In this case, each energy-dissipating mechanism must be appropriately accounted for in the cohesive law.

Several failure mechanisms, including fiber tensile fracture, fiber-matrix pullout and matrix cracking are present when a crack propagates in a plane perpendicular to the fiber direction. It was demonstrated by Dávila *et al.* [16] that a simple bilinear law is unable to predict the load displacement response obtained in a cross-ply compact tension test. A tri-linear law was proposed, with parameters of the softening law determined from the experimentally determined *R*-Curve, using the procedure defined by Dávila, *et al.* The load-displacement response observed in the test was successfully predicted when the determined softening law was used in a simulation that represented the specimen fracture with cohesive elements embedded in the model along a fracture plane extending from the initial notch tip.

Predictions obtained with the softening law incorporated in the continuum damage mechanics model, however, were not as successful. Preliminary simulation results, shown in Fig. 5 predict the development of splitting cracks parallel to the 0-degree fibers fairly early in the loading. The

cracks develop over large portions of the coupon, and are not constrained to the immediate vicinity of the idealized fracture surface. These cracks likely developed in the test as well, however, their presence is not explicitly noted, and their contribution to the measured  $R$ -curves is not clear. The possible presence of these splitting cracks in the compact tension specimens affects both the total energy dissipated into the creation of new fracture surfaces and the severity of the stress concentration ahead of the notch. Furthermore, the measured fiber fracture toughness becomes dependent on the matrix properties and stacking sequence of the cross-ply specimens.

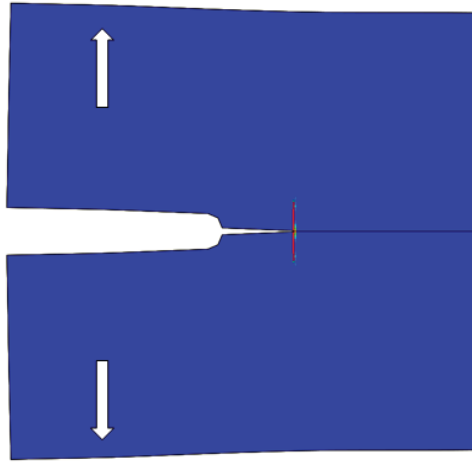


Fig. 5. Matrix splitting predicted via CDM in a compact tension finite element model.

Results of these simulations illustrate the difficulty in properly interpreting the experimental data, and backing out the necessary input for the damage models. As more and more detail and fidelity in representing evolving damage mechanisms are incorporated into the damage models, care must be taken to prevent double-counting the contributions of individual energy dissipating mechanisms. Experimental studies with detailed NDE examination, including in-situ ultrasound, and X-Ray/CT during interrupted tests, to examine the evolution of all of the damage modes during the coupon loading, coupled with high-fidelity analysis are required to resolve these issues. To this end, several compact tension specimens, with varying stacking sequences would be required to decouple the measured fiber fracture toughness from the specimen configuration dependencies. New NDE techniques with resolution sufficient to capture fiber failures and fiber-matrix debonding may be required as well to provide sufficient characterization of all of the significant damage modes and their interactions.

Determining the fracture toughness for longitudinal failure in compression is more challenging. Compact compression tests were previously proposed to be a good configuration for measuring resistance curves associated with fiber kinking. However, delamination that accompanies the propagation of a kink-band renders the compact compression test unsuitable for this purpose. Test specimen and experimental design are required to determine the fiber fracture toughness in compression.

***In-Situ Strengths and Shear Nonlinearity.*** To predict matrix cracking in a laminate subjected to in-plane shear and transverse tensile stresses, a failure criterion must account for the ‘in-situ’ strengths. Within multidirectional laminated composites, laminar strength oftentimes does not correspond directly to the experimentally measured strengths of a unidirectional composite. Adjoining plies of differing orientations constrain the laminae, affecting their effective strength. These in-situ strengths vary with the unidirectional strength, fracture toughness, and thickness of

the individual plies. The in-situ effect, originally detected in Parvizi's [48] tensile tests of cross-ply glass fiber reinforced plastics, is characterized by higher transverse tensile and shear strengths of a ply in a laminate when it is constrained by plies with different fiber orientations, compared with the strength of the same ply in a unidirectional laminate. The in-situ strength also depends on the number of plies clustered together, and on the fiber orientations of the constraining plies. The results of Wang's [49] tests of  $[0/90_n/0]$  carbon-epoxy laminates indicate that thinner plies exhibit higher transverse tensile strength.

The in-situ strengths have been solved for by Camanho and Dávila for both matrix tensile and shear modes [50]. Due to the different fracture mechanisms acting on plies of different thicknesses and at different positions within a laminate, different in-situ strength equations were developed for thin embedded, thick embedded and surface plies. For the case of thin embedded plies, the general equation used to solve for the in-situ strength is:

$$G_c = \frac{\pi t}{4} \int_0^{\varepsilon_{\text{ult}}} \sigma d\varepsilon \quad (3)$$

where  $G_c$  is the fracture toughness,  $t$  is the ply thickness, and  $\varepsilon_{\text{ult}}$  is the strain corresponding to the unidirectional strength of the material. Using equation (3), all strain energy preceding failure (both elastic and inelastic) is related to the corresponding experimental fracture toughness of the material through a fracture mechanics analysis of a constrained ply. In-situ strengths are found to have an inverse relationship with ply thickness (or the number of plies blocked together), increasing with decreasing thickness. The in-situ strength for thick embedded plies, however, is constant, not scaling with thickness.

Several continuum damage mechanics models have been proposed that either neglect shear nonlinearity or provide the end-user with the ability to ignore the effects of shear nonlinearity in their particular model. The simplification of neglecting shear nonlinearity, however, is at odds with the use of in-situ shear strengths. Shear nonlinearity is integral to the current derivation of in-situ shear strengths [50], and electing to neglect shear nonlinearity while utilizing in-situ shear strengths is contradictory.

For example, as currently derived, in-situ shear strengths are highly dependent on the shape of the shear stress-strain response (e.g., linear vs. nonlinear) prior to failure. To avoid adopting contradictory assumptions, it is necessary to model the nonlinear shear behavior in the manner that is assumed during the derivation of the in-situ shear strengths. Furthermore, much effort has been devoted to properly evolving the state of matrix damage throughout the full range of possible mode mixities (see below). Even moderate amounts of shear nonlinearity can have a considerable influence on the calculated mode mixity for a given strain history, causing drastic changes in the effective toughness of the local material and the overall strength of the modeled structure.

In their original derivation of in-situ shear strengths, Camanho and Dávila utilized a shear nonlinearity equation by Hahn and Tsai in which a single parameter is used to fit experimental shear data [51]. However, this equation was found by Schuecker, *et al.* [52] to lack the necessary flexibility to closely match all experimental shear responses. In order to maintain flexibility in the shape of the shear response curve, the two-parameter Ramberg-Osgood law [53] was selected to represent the nonlinear shear response:

$$\gamma_{12} = \frac{1}{G_{12}} \left[ \tau_{12} + \alpha_{\text{pl}} \text{sign}(\tau_{12}) |\tau_{12}|^n \right] \quad (4)$$

where  $\alpha_{\text{pl}}$  and  $n$  are used to fit experimental shear data. A comparison of the abilities of the Hahn-Tsai and Ramberg-Osgood laws to fit experimental shear data from the second World-Wide Failure Exercise is shown in Fig. 6. Clearly, the added flexibility of the Ramberg-Osgood law allows for a much better approximation of the experimental data.

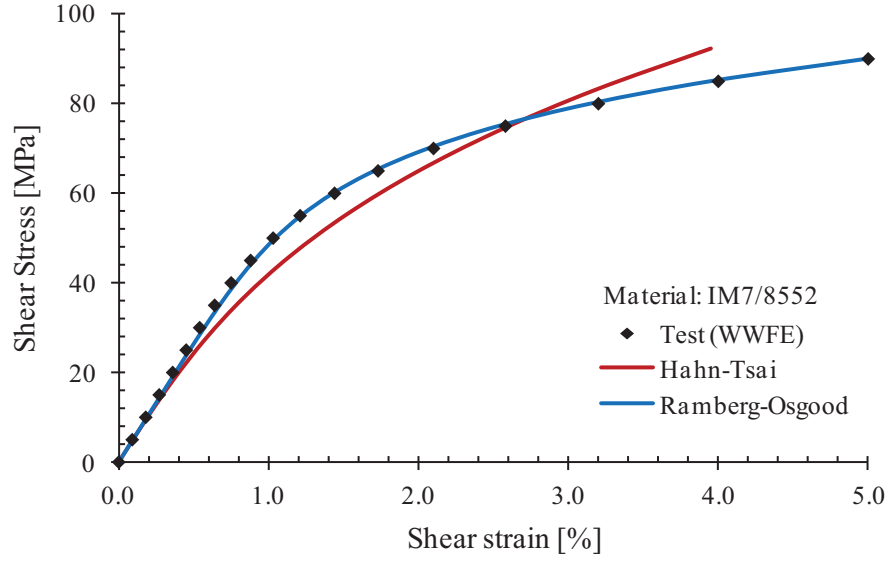


Fig. 6. Comparison of the Hahn-Tsai and Ramberg-Osgood shear nonlinearity equations with experimental shear data from the second WWFE. For the Hahn-Tsai curve,  $\beta$  is equal to  $2.80\text{E}-8$ ; for the Ramberg-Osgood curve,  $\alpha_{pl}$  and  $n$  are equal to  $4.41\text{E}-10$  and  $5.93$ , respectively.

The use of the Ramberg-Osgood shear law in place of the Hahn-Tsai law required that the in-situ shear strengths be re-derived. The primary difference between the Ramberg-Osgood and Hahn-Tsai laws is the replacement of the cubic exponential term with the variable exponent  $n$ . The inclusion of this a priori unknown exponent  $n$  causes there to be no closed-form solutions for the in-situ shear strengths. The Newton-Raphson method is used to obtain an approximate solution for the in-situ shear strength  $S_{L, is}$  by solving equations (5) through (7) when the equations are equal to zero:

$$\text{Thin Inner Plies:} \quad f(S_{L, is}) = \frac{4G_{12}G_{IIc}}{\pi t} - \frac{S_{L, is}^2}{2} - \frac{\alpha_{pl}n}{n+1} S_{L, is}^{n+1} \quad (5)$$

$$\text{Thick Inner Plies:} \quad f(S_{L, is}) = \left( \frac{S_{L, is}^2}{2} + \frac{\alpha_{pl}n}{n+1} S_{L, is}^{n+1} \right) - 2 \left( \frac{S_L^2}{2} + \frac{\alpha_{pl}n}{n+1} S_L^{n+1} \right) \quad (6)$$

$$\text{Surface Plies:} \quad f(S_{L, is}) = \frac{2G_{12}G_{IIc}}{\pi t} - \frac{S_{L, is}^2}{2} - \frac{\alpha_{pl}n}{n+1} S_{L, is}^{n+1} \quad (7)$$

An example of the predicted variation of the in-situ shear strengths with ply thickness for an embedded ply of IM7/8552 is shown in Fig. 7, using three different pre-failure shear responses: linear, Hahn-Tsai, and Ramberg-Osgood. Clearly, the in-situ shear strengths are highly sensitive to the posited shape of the shear response, with the in-situ strength decreasing with increasingly nonlinear responses. Also worth noting is the much lower transition between the thick and thin ply regions: for the case of the Ramberg-Osgood law fit to the WWFE data, a single 0.125-mm thick ply of IM7/8552 is considered thick, and, therefore, the strength is not predicted to scale with ply blocking.

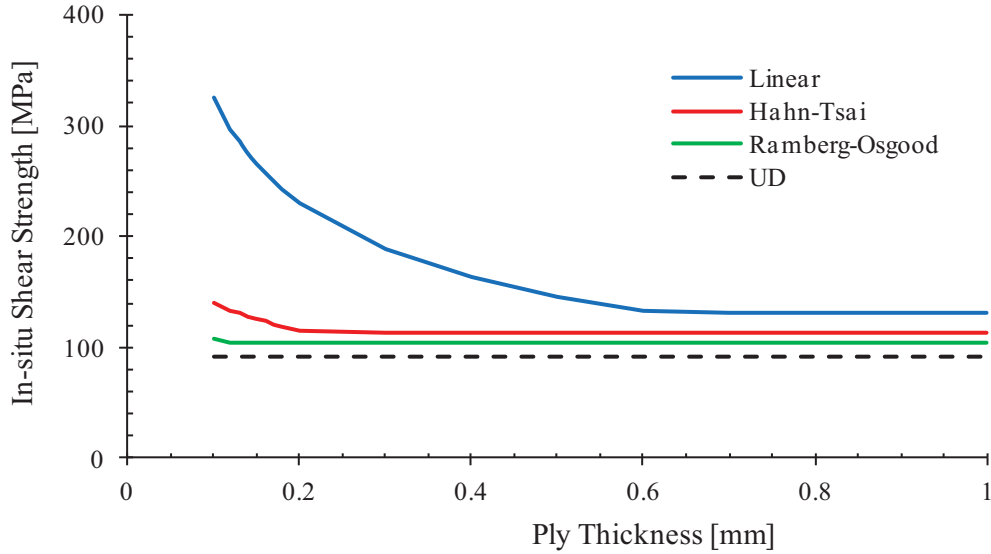


Fig. 7. In-situ shear strengths for IM7/8552, as a function of ply thickness. The corresponding unidirectional shear strength is 92.3 MPa.

For a material with a given fracture toughness, the low in-situ shear strengths corresponding to highly nonlinear material responses lead to very high in-situ ultimate strains. For example, a single embedded 0.125-mm thick ply of IM7/8552 will have in-situ ultimate strains of 5.5%, 8.9% and 9.8% using the linear-elastic, Hahn-Tsai, and Ramberg-Osgood shear laws, respectively. For the case of thin-ply laminated composites (e.g., 0.04-mm thickness) [54], these strains increase to 9.7%, 19.7%, and 24.6%. These strain values are far beyond the experimental unidirectional results (approximately 5% for IM7/8552). It is expected that extrapolations of the nonlinear shear response curves are invalid at these very high strains. Without further experimental data demonstrating the relationships between nonlinear shear behavior and in-situ shear strengths in various laminate configurations, the reliability of predicted in-situ shear strengths is questionable.

The significant dependence of in-situ shear strengths on the assumptions made regarding the shape of the nonlinear shear stress-strain response highlights the importance of maintaining consistency between the selection of in-situ shear strengths and the assumed shear behavior for a particular model. Furthermore, a greater understanding of the nonlinear shear response of IM7/8552 is required, including, but not limited to, its dependence on the in-situ effect and on transverse loading.

### 2.2.2 Limitations of Continuum Damage Mechanics Models

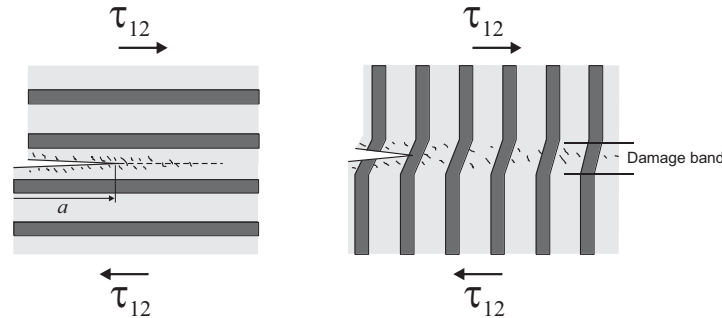
Despite advances in progressive damage modeling, recent studies [10, 11] indicate that CDM models coupled with cohesive zone models may not always represent laminate failure sequences properly. These deficiencies are particularly evident when the observed fracture mode exhibits matrix splitting and pullouts [55] or when the fracture is characterized by a strong coupling between transverse matrix cracking and delamination. The deficiencies of the predictive capabilities consist of several issues, including the incorrect prediction of the damage zone size normal to the fracture direction when using crack-band models and the inability of local CDM models to reliably predict matrix crack paths. These limitations are mostly due to the fact that CDM models are usually implemented as “local” rather than “non-local” models [56], i.e., the evolution of damage in a local CDM is evaluated at individual integration points without

consideration of the state of damage at neighboring locations. The following discussion pertains mostly to such local implementations, since non-local damage models are less widely used due to the difficulty in implementing them within the finite element method.

The premise of the crack-band approach for regularizing CDM models is that damage localizes into a band with a width equivalent to the element dimension. If the element size is smaller than the damage process zone, the crack-band approach may not predict correctly the width of the damage zone nor the local stress field. Consequently, the stress redistribution resulting from damage development may be inaccurately predicted and can potentially result in inaccurate representation of damage mode interactions and failure sequences.

As a result of homogenization and damage localization, CDM models have difficulty predicting crack paths. Since homogenization eliminates the distinction between fibers and matrix, a CDM model cannot distinguish between cracks that propagate along fiber directions from those that cross fibers when loaded in shear [10]. In CDM models implemented with damage localization, the damage state at any integration point in the model depends only on the stress field at that point rather than the damage state of neighboring points. Therefore, the direction of damage evolution is driven only by the instantaneous local stress distribution. In other words, the local direction of cracking may be predicted correctly by the failure criteria, but the sequence of failures that eventually defines the path of a crack at a macroscopic level may be predicted incorrectly.

The inability of CDM models to determine the correct direction of propagation is particularly evident when the stress field is dominated by shear. Consider two different plies in a laminate with a notch and subjected to shear, as shown in Fig. 8. In both situations, the direction of the matrix microcracks is correctly predicted by the failure criterion to be  $45^\circ$ . Furthermore, both situations would result in an identical sequence of failures, since the stress field is identical. However, it is clearly not the same to propagate a crack in a sequence of linked microcracks (Fig. 8a) as it is to propagate a crack band across fibers (Fig. 8b). Matrix cracking in a shear band running parallel to the fibers is a relatively brittle failure mechanism, whereas matrix cracking normal to the fibers produces a damage band that requires much more work to propagate.



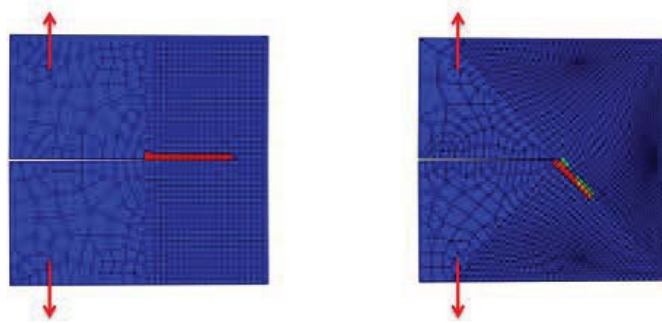
a) Propagation of shear damage along fiber      b) Propagation across fiber direction

Fig. 8. Idealized propagation of shear damage (adapted from [10]).

The sensitivity of CDM predictions to the finite element mesh orientation also contributes to the difficulty in predicting the crack path. Although the objectivity of the solution with respect to element size is addressed with the crack-band approach described previously, the predicted damage may be dependent on mesh orientation and element shape. When strain-softening constitutive models are used in a finite element simulation, damage tends to propagate along preferred directions, consisting of either element edges or element diagonals. A demonstration of the sensitivity of simulation results to mesh orientation is provided in Fig. 9 for a unidirectional compact tension specimen with the fiber placed at  $90^\circ$  to the load direction. Results are presented



for simulations obtained with a mesh oriented parallel to the fiber direction (Fig. 9a) and with an inclined mesh in front of the crack tip (Fig. 9b). The crack should propagate along the fiber direction. However, the results show directional bias, and the simulated crack band propagates in the direction of the element alignment.



a) Mesh aligned with crack direction    b) Mesh inclined to crack direction

Fig. 9. Effect of mesh orientation on crack path in a unidirectional CT specimen.

The tendency for damage to localize along mesh lines can be partially attributed to shear locking [56]. In the CDM methodology, a crack or displacement discontinuity is represented by a degradation of the corresponding terms in the constitutive stiffness. As the crack opens, the stiffness degradation is such that stress should not be transferred across the crack faces. However, such unloading may not occur due to in-plane shear locking. Shear locking here refers to inappropriate shear stress transfer across a widely open smeared crack, which occurs when an element cannot shear without inducing tensile strains. In a ply with orthotropic properties, a matrix crack should be represented by setting the transverse shear modulus,  $G_{12}$ , and the transverse Young's modulus,  $E_{22}$ , to zero. However, quadrilateral elements have been shown to exhibit coupling between  $\gamma_{12}$  and  $\varepsilon_{11}$  unless the element edges are aligned with the softening band or are oriented at 45 degrees to the band [56]. Furthermore, the tendency of the element to lock is dependent on the order of integration of the element: fully integrated elements are more susceptible to pathological in-plane shear locking than reduced-integration elements. The shear stress transfer across an open smeared cracked can result in inaccurate prediction of stress redistribution after damage development.

Load transfer across CDM cracks is also related to the complexity of representing the kinematics of a fully or partially damaged material with a single integration point. CDM models are implemented at the integration point level. Typically, a single integration point is used to represent the constitutive response of a single material. After the local initiation of damage, however, an integration point is tasked with representing the evolution of a crack and the constitutive responses of the bulk material on each side of the crack. While the local stress terms that are normal to and acting on the new crack plane will be equal in each of these three material sections, the stress terms acting parallel to the crack plane in the remaining bulk material will be artificially linked due to their shared integration point. Ideally, the stress terms parallel to the CDM crack could be solved for and stored separately for the material on either side of the crack, similar to two solid elements with a cohesive element in the middle.

When damage localizes and a fracture path is known *a priori*, a relatively simple approach to circumvent some of the limitations of CDM models noted above consists of aligning the mesh with the direction of fracture [57] to force a matrix crack to localize along the fiber direction. The benefit of mesh alignment was demonstrated by Song *et al.* [58] for a 0-degree unidirectional

open-hole tension specimen, loaded parallel to the fibers, and in quasi-isotropic open-hole tension specimens whose failures were dominated by development of matrix and delamination cracks.

Predictions obtained with aligned meshes were significantly improved over those obtained with a traditional radial mesh, and demonstrated an ability to predict properly crack paths, and failure sequences, where predictions obtained with traditional radial meshes were unsuccessful. However, the lack of kinematic freedom within a simulated crack represented by a band of softened elements prevented total stress relaxation across the open crack, leading to some inaccuracy in calculations of stress redistributions. Additionally, use of structured meshes corresponding to the fiber orientation in each ply to describe properly matrix cracks and thus reduce mesh dependency, leads to non-coincident meshes through the laminate thickness. Tie constraints are therefore required to connect the individual plies in a finite element model. The use of tie constraints results in large run times and computational resource requirements, which may render these types of models intractable for large applications.

### 2.2.3 Refinements to CDM Models

In addition to developing modeling approaches for addressing some of the deficiencies in CDM approaches for representing matrix and delamination cracking interaction, significant effort has been devoted to refining the continuum damage mechanics (CDM) finite element (FE) subroutine (LaRC CompDam CDM software [59]) corresponding to the damage model originally proposed by Maimí [36].

***Refinements to Continuum Damage Mechanics Model.*** The first modification addresses deficiencies in the CDM model presented in [36], for predicting crack propagation. The CDM model used separate matrix tension (or compression) and shear damage state variables to affect the damaged material response, each of which were functions of only the elastic limit. That is, as the evaluated mixed-mode failure criterion increased in value, the evolution of the damage variables was independent of the local mode mixity. A new mixed-mode matrix damage evolution law has been developed, based on the cohesive zone damage model of Turon [25]. In the updated CDM model a single matrix tension (or compression) and shear damage variable is used, defined using mixed-mode properties corresponding to the ratio of the transverse and shear strains [59].

In addition to the new matrix damage evolution law, changes have been made to the stresses which drive damage evolution and to the shape of the nonlinear shear responses prior to the onset of damage that can be modeled. Within the CDM model, a combination of the LaRC03 [39] and LaRC04 [40] failure criteria are used to drive the development of the damage state variables. These failure criteria are evaluated in terms of their *effective stress*. These effective stresses are representative of the stress state in the intact cross-sectional area of the element, and can accurately drive damage from onset to complete failure while a single damage mode is present. As was noted by Schuecker [52], however, the subsequent initiation and development of additional damage variables can lead to erroneous results with the current definition of effective stresses. To address this issue, the development of each damage variable is defined in terms of all other damage variables. For example, the effective stresses that drive the formation of the fiber damage variables consider the current matrix damage state, and the effective stresses that drive the formation of the matrix damage variables consider the current fiber damage state. This revision of the effective stresses removes the potential for spurious additional damage modes to be predicted and allows for a more accurate simulation of multiple simultaneous local damage mechanisms.

The presence of any plasticity and/or damage at an integration point can lead to very large strains in a still partially intact volume of material. In order to properly represent the deformed material and the orientation of any local fracture surfaces while under finite strains, the LaRC



CompDam CDM software has been updated to perform all stress and strain calculations in terms of the 2<sup>nd</sup> Piola-Kirchhoff stress tensor and the Green-Lagrange strain tensor.

***Smearred Crack Formulation for Representing Matrix Cracks.*** An alternate formulation of the CDM model has also been developed that includes an embedded cohesive law for the representation of matrix damage within a continuum finite element, based on the smeared crack formulation of Camanho, *et al.* [60]. The goal of this implementation is to represent accurately the formation, opening, and closure of matrix cracks in fiber-reinforced composite materials under large deformations by improving the kinematics of cracked material. If matrix cracks are represented solely by softening certain terms of the constitutive stiffness matrix of damaged elements, the determined orientation of cracks within damaged elements becomes increasingly erred when the elements undergo large shear deformations. An incorrectly determined crack normal causes elements containing matrix damage to “collapse” normal to the fracture plane when under shear load, and contributes to spurious load transfer across the fracture plane due to the fiber direction being incorrectly influenced by the elemental shear. The inclusion of the embedded cohesive law provides improved bulk material stress and strain predictions, as well as improved predictions of crack opening or closure displacements under large shear deformations.

To accomplish this goal, it is necessary to : i) establish the orientation of the crack; ii) develop a consistent means of describing the bulk and cohesive deformations in terms of the elemental deformation; and iii) determine the distribution of elemental deformation between the bulk and cohesive materials. The implementation is carried out by decomposing the elemental deformation gradient tensor into two parts: a new deformation gradient tensor associated with only the bulk material, and a displacement vector describing the cohesive displacement-jump. The orientation of the cracks is defined according to the bulk material deformation gradient tensor. The distribution of deformation between the bulk and cohesive domains is determined by considering the current stiffnesses of the two materials. Stress equivalence on the rotated fracture plane is assumed, and the Newton-Raphson method is used to solve for the distribution of bulk and cohesive displacements whenever there is a predicted change in the damage state.

An example of the improved predictive capability offered by the smeared crack formulation is shown in Fig. 10, for a unidirectional open-hole tension specimen. While the accurate prediction of matrix cracks (Fig. 10a) is possible with traditional CDM methods, problems arise after continued stretching of the specimen, including nonphysical contraction normal to the fracture plane and increasing load transfer across the fracture plane with continued shear deformation. Using the cohesive-embedded CDM model, there is no increasing component of stress transfer across the matrix splits (Fig. 10b and Fig. 10c), and the deformation normal to the matrix fracture plane is maintained (Fig. 10d).

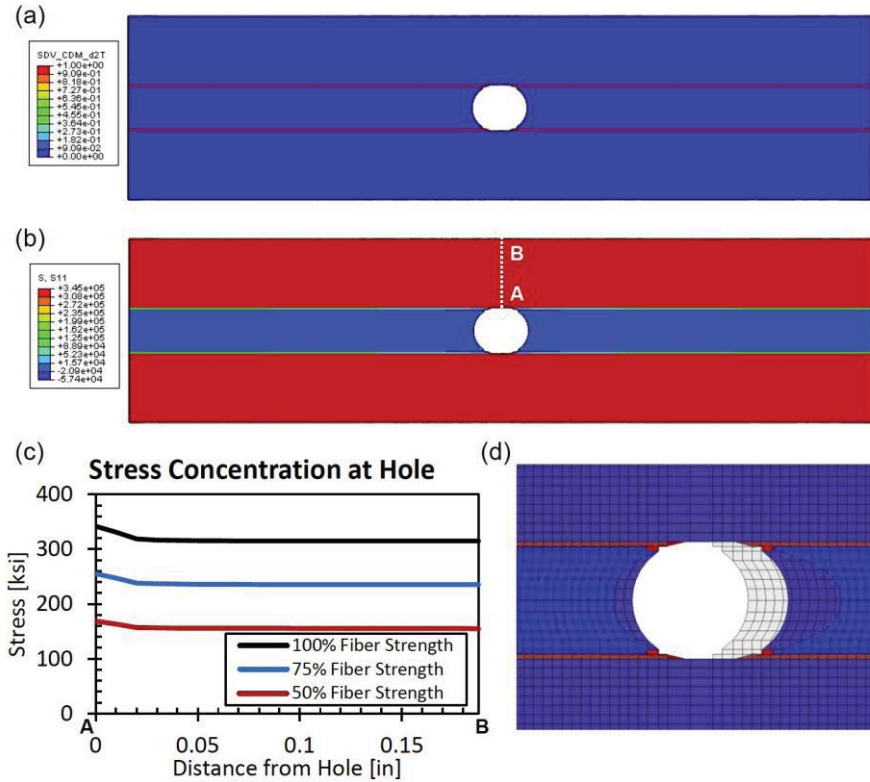


Fig. 10. Open-hole tension finite element model results: (a) matrix damage; (b) fiber stress; (c) constant stress concentration factor with increasing elemental shear deformation ( $\sim 1.08$ ); and (d) cracked element deformation under high shear deformation.

## 2.2.4 Summary, Continuum Damage Mechanics Models

### 2.2 Continuum Damage Mechanics Models

#### State of the Art

- CDM models that use failure criteria and regularized softening laws can predict the initiation and propagation of intralaminar damage modes.
- CDM is an improvement over Progressive Failure Analysis, which is mesh-dependent.

#### Recent Advances

- Progress made in identifying and addressing the limitations of CDM.
- Improvements made to LaRC CompDam CDM software, include: use of 2<sup>nd</sup> Piola-Kirchhoff stress tensor and deformation gradient; embedded cohesive crack within bulk continuum, new definition of effective stresses; improvements in mixed-mode matrix cracking prediction.

### **Technology Barriers**

- *Experimental characterization must be capable of separating different toughening mechanisms such as notch blunting by fiber bridging from fiber fracture according to the kinematic complexity of the model.*
- *Convergence rate of nonlinear solution in implicit analyses*

### **LaRC CDM Research Software**

- *CompDam\_UMAT.06 (LaRC, P. Maimí, U. Girona, [6, 43])*
  - *Continuum Damage Model for laminated composites based on the LaRC03 damage activation functions [39].*
  - *Two-part linear/exponential softening for fiber damage, exponential softening for all other damage modes.*
  - *User-written UMAT subroutine for Abaqus/Std.*
- *CompDam\_UMAT.10 (LaRC, P. Maimí, U. Girona, unpublished)*
  - *Bilinear softening laws of fiber tension and fiber compression.*
  - *Linear softening laws for matrix tension and matrix compression.*
  - *Simple plasticity model in inplane shear*
  - *New multi-mode damage variable for postprocessing.*
- *CompDam\_VUMAT.13 (LaRC, unpublished)*
  - *Damage-mode-dependent effective stresses for proper evolution of multiple simultaneous failure processes.*
  - *Finite strain and stress formulation used for representing wide-open cracks.*
  - *Mixed-mode matrix crack softening.*
  - *Improved shear plasticity modeling.*
  - *Transverse shear plasticity.*
  - *Implemented as a VUMAT subroutine for Abaqus/Explicit.*

## **2.3 Discrete Damage Modeling Methods**

The eXtended Finite Element Method (X-FEM) is a technique that can be used to predict the location and evolution of matrix cracks in composites while avoiding the aforementioned limitations associated with continuum damage mechanics models. X-FEM is a mesh enrichment technique based on a pioneering concept by Moës [61] that facilitates the introduction of displacement discontinuities such as cracks at locations and along directions that are independent of the underlying finite element mesh. Although most of the research on X-FEM is devoted to arbitrary crack propagation in isotropic materials, recent applications to composite materials include delamination modeling and textile composite architecture representation [62, 63]. Huynh [64] provides a review of contemporary development of X-FEM, as well as novel applications to interfacial cracking analysis in two- and three-dimensional problems.

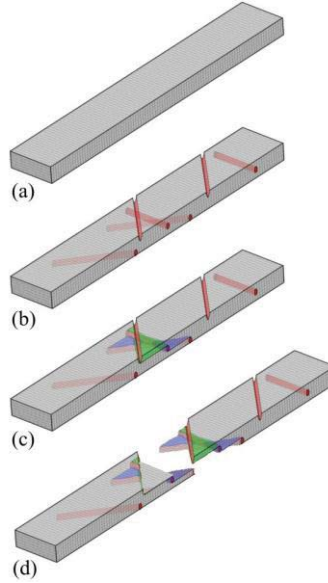


Fig. 11. Matrix crack and delamination interactions in a composite laminate: (a) initial stage without damage, (b) matrix cracking stage, (c) delamination stage, linking up of matrix cracks in various plies, (d) specimen fracture [72].

Modeling a matrix crack in a ply that propagates parallel to the ply fiber direction is conceptually straightforward using X-FEM. However, it is more difficult to model networks of matrix cracks in a laminate where the fracture planes of matrix cracks in individual plies intersect at common interfaces and can cause delaminations that link the cracks through the thickness, as shown in Fig. 11. Within the traditional X-FEM approach, the difficulty in modeling networks of linked matrix cracks could be addressed by developing a special enrichment for multiple crack situations or by connecting two enriched/cracked elements. Such connection was recently accomplished in a quasi-two dimensional formulation by van der Meer et al. [65] and Ling et al. [66].

Another direction in which the X-FEM is being developed is the regularized extended finite element method (Rx-FEM) proposed by Iarve [67-70]. In the Rx-FEM approach, the usual step function used in X-FEM approaches to describe the crack surface is replaced by a continuous function. Displacement shape functions are used to approximate the step function, and the Gauss integration can be retained for element stiffness matrix computation regardless of the orientation of the crack. The cohesive connection between two plies in which matrix cracks have been introduced can then be easily established by computing integrals of the products of the shape functions at the ply interface. Therefore, a kinematically powerful model of crack networks can be constructed in which transverse matrix cracks parallel to the fiber direction are inserted with the Rx-FEM technique at locations determined using a failure criterion. A cohesive interface damage model is used to represent matrix crack propagation and delamination between plies [71].

Preliminary validation studies of X-FEM methodologies for un-notched and notched laminates subjected to tensile loading have demonstrated high fidelity in predicting experimentally observed responses, indicating the potential of this methodology [2-4, 71, 72]. An example of the predictive capability of the Rx-FEM approach developed by Iarve *et al.*, is shown in Fig. 12 for a laminated composite Overheight Compact Tension (OCT) specimen [2]. Predicted damage patterns shown on the left are compared with measured X-Ray/CT data [73] on the right for a  $[45_2/90_2/-45_2/0_2]_s$  specimen loaded to a pin-opening displacement (POD) of 2.55 mm. The damage patterns shown in the figures are a superposition of all cracks (black in Fig. 12a, and white in Fig. 12b) and all delaminations (blue, green and orange) through the specimen thickness.

A comparison of the predictions and experimental results shows very good correlation between the simulated and experimental delamination shapes and extent, and the matrix cracking distribution.

### 2.3.1 Mesh Sensitivity/Refined Cohesive Elements for Proper Interaction

Adopting a modeling approach as described above with the ply material modeled with advanced X-FEM elements to allow for arbitrary cracking, and cohesive elements at ply interfaces to account for potential delaminations, should ideally provide a direct coupling between developing ply cracks and interface cracks. However, when a discontinuity is inserted in the displacement field of a plane element that is connected to a cohesive interface element, the relative displacement between the planes is affected. Allowing a solid element representing a ply to crack, theoretically requires the interface element connected to the cracked ply to be modified accordingly to ensure proper stress transfer across the interface. Additionally, the possibility that cracking has occurred in elements above and below the interface plane should be accounted for.

To address this issue, an augmented cohesive zone (ACZ) element has recently been proposed that is based on the augmented finite element (A-FEM [66]) formulation to allow for arbitrary separation of the cohesive element in accordance with the separations that have occurred in adjacent solid elements [74]. The effectiveness of the proposed ACZ elements has been demonstrated for several sample problems. However, the additional complexity in the numerical models may not be required. Standard non-augmented interface cohesive elements may be sufficient for most applications, especially when using fine meshes [71, 75]. Additional studies are required to better understand the modeling requirements and to validate modeling assumptions.

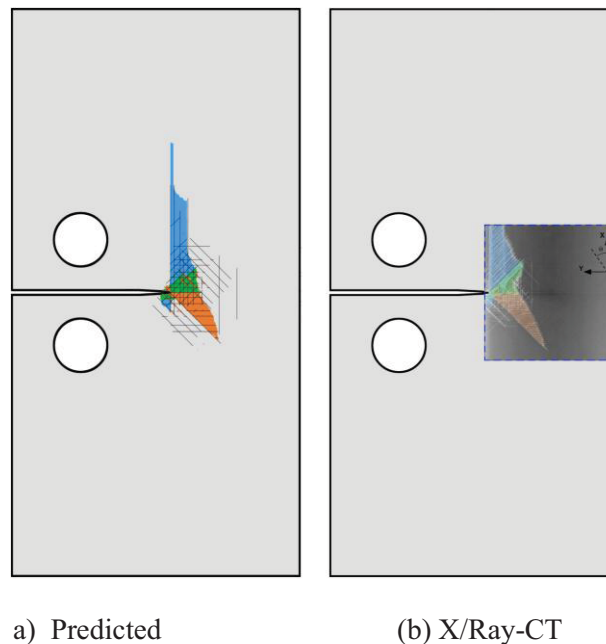


Fig. 12. Superposed predicted and experimental cracking and delamination extent for a  $[45_2/90_2/-45/0_2]_s$  compact tension specimen loaded to a POD of approximately 2.55 mm. (From Mollenhauer [2], with permission)

### 2.3.2 Crack Initiation, Saturation and Delamination Onset

Failure analyses with X-FEM are most often performed at the meso-scale level, in which each ply is represented by a homogeneous orthotropic material. To capture the proper sequence of load redistributions that result from interactions between matrix cracks and delaminations, each ply must be modeled with separate elements. Therefore, the minimum mesh requirement consists of a single layer of elements across the thickness of each ply and a layer of cohesive elements between the plies. Few analyses have been attempted with more than one element over the thickness of the ply because the computational requirements associated with such small elements render intractable any analysis larger than a small coupon. However, the elliptical opening profile of a transverse crack cannot be represented with a single element, as illustrated in Fig. 13, for a cross-ply  $[0/90_n/0]$  laminate, loaded in tension parallel to the 0-degree fibers. Studies have been initiated to investigate the ability of meso-scale level X-FEM models with a single layer of elements per ply to capture accurately all aspects of matrix cracking. In particular, whether the models can predict the in-situ ply thickness effect on crack initiation and propagation, the crack density as a function of strain, the strain for crack saturation, and the interaction between delamination and transverse cracks are being assessed.

In collaboration with F. van der Meer, TU Delft, it has been shown for the first time that initiation and propagation of transverse matrix cracks in composite laminates can be captured with cohesive zone analysis [76]. Experimental results show that the load levels at which the cracks grow in the transverse direction increase with decreasing thickness of the ply, a trend which is correctly predicted by the cohesive model. It was shown that a second critical load level exists which is associated with propagation in the thickness direction. For thin plies, the in-situ strength is governed by transverse propagation, while through-thickness propagation is critical for thick plies.

Stress relaxation due to crack opening plays an important role in the transverse crack propagation, which governs the thin ply in-situ strength. This crack opening cannot be captured when only one element is used through the thickness of a ply and the interface between plies is rigid prior to delamination onset. However, a technique based on shear lag was introduced which makes the interface deformable. Crucial for a proper prediction of the in-situ effect is that the stiffness of the interface is inversely proportional to the thickness of the transverse ply. The required interfacial properties were determined analytically using a closed-form shear lag model. As a result, the dependence of the propagation load level on the thickness can be captured with a cohesive method with a single element per ply. Preliminary results indicate that this modified model can also capture the density of transverse matrix cracks as a function of the applied strain. Additional work is necessary to ensure that the interfacial compliances do not adversely affect the softening response of the interfacial cohesive elements.

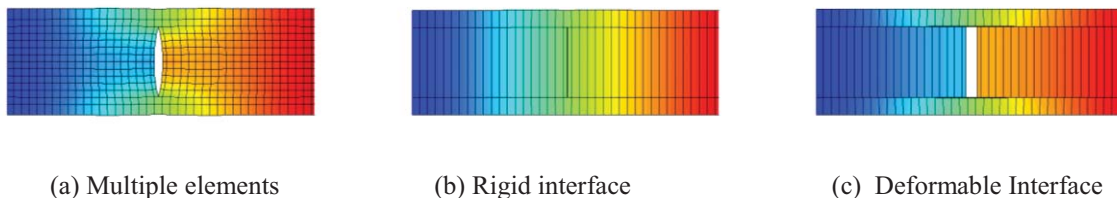


Fig. 13. Side view of final deformation for three different cases: multiple elements across the thickness (a), single element with rigid interface (b) and single element with deformable interface (c); shading indicates displacement in load direction.



### 2.3.3 Extensions for Compression after Impact and Fatigue Loading

The initial development of the X-FEM methodologies focused on modeling transverse matrix crack and delamination interaction for tension loading. Fiber failures were not considered. Preliminary validation studies for un-notched and notched laminates subjected to tensile loading have demonstrated high fidelity in predicting experimentally observed responses, indicating the potential of this methodology [2-4, 71]. NASA currently has a grant with the University of Dayton Research Institute (UDRI) to extend the methodology to include tensile fiber damage, matrix cracks that are inclined through the thickness of a ply, as develop in certain combinations of shear and compression loading, and fatigue loading conditions. Additional extensions required to address the problem of predicting damage due to impact include accounting for geometrically non-linear deformations, and transient loading conditions. Extensions to address the prediction of compression after impact strength include, as a minimum, coupling with a CDM model to include the effects of fiber on the compression failure.

Additional development of the fatigue constitutive model described above is required to ensure that the same model can predict transverse matrix cracks within the X-FEM framework as well as delamination propagation in cohesive element models. For fatigue loading, material characterization testing will be required and may include additional Paris law coefficients, S-N curves, etc. Additionally, pathfinder experiments are required for both compression loading and fatigue loading to guide the model development, to determine the critical phenomena that must be modeled and at what scale.

### 2.3.4 Summary, Discrete Damage Models

<p><b>2.3    <i>Discrete Damage Models</i></b></p> <p><b><i>State of the Art</i></b></p> <ul style="list-style-type: none"><li>• <i>X-FEM modeling techniques are gaining wider acceptance. Commercial FEM vendors such as DS-Simulia/Abaqus and ANSYS are developing X-FEM capabilities.</i></li><li>• <i>Current commercial capability usually allows a single crack in a domain, which is insufficient for composite analysis.</i></li><li>• <i>Majority of formulations are two-dimensional; bending deformations are not included.</i></li><li>• <i>Predictive capability demonstrated for limited applications subjected to monotonic tension loading.</i></li></ul> <p><b><i>Recent Advances</i></b></p> <ul style="list-style-type: none"><li>• <i>LaRC has spurred the development of two X-FEM modeling techniques (A-FEM and Rx-FEM) that are capable of predicting complex crack networks in laminated composites and the failure that results from the interactions of the cracks and delaminations.</i></li></ul> <p><b><i>Technology Barriers</i></b></p> <ul style="list-style-type: none"><li>• <i>Methods are needed to predict matrix cracking and the associated in-situ effects with a single element per ply.</i></li></ul>
---

- *X-FEM models are not capable of predicting fiber failure. Hybrid X-FEM/CDM models are needed.*
- *Extensions are required for compression damage, and for fatigue loading.*
- *Computational requirements limit application to small specimens. Methods for coupling with continuum representations are required.*

**LaRC DDM Research Software**

- *BSAM (U. of Dayton Research Institute (UDRI), LaRC, [71])*
  - *Regularized extended finite element model for laminated composites based on X-FEM*
  - *Mixed-mode bilinear cohesive laws for matrix crack and delamination propagation [29], LaRC03 failure criteria for matrix crack insertion [39], and CompDam CDM model [6, 43].*
  - *Stand-alone analysis code and VTMS post-processor*
- *A-FEM\_UEL.10 (U. of Miami, Teledyne Scientific, LaRC [66])*
  - *Augmented-FEM approach based on X-FEM and extended to laminated composites.*
  - *User-written UEL for Abaqus/Std.*

### 3 Experimental Methods

Recent advances in damage mechanics have led to increasingly complex models of damage evolution in composite structures with vast numbers of new computational models capable of predicting the damage processes in composites continuously being advocated. However, major challenges remain to improve the quantitatively predictive power available to the engineer today through these unprecedented computational/analytical techniques. The process of improving predictive capability requires a close interaction between experimentalist and theories to ensure that the basic building blocks of the theories are well established.

In the past five years there has been significant interaction with the Nondestructive Evaluation Sciences Branch (NESB) at NASA Langley Research Center (LaRC) to use existing NDE techniques and to develop new experimental capability within the structural and materials laboratories to allow for detailed pre- and post-test inspection of test specimens, as well as inspection under load. Routine examinations prior to all tests include accurate measurement of surface geometry using coordinate measurement machines, and ultrasonic inspection to provide an indication of specimen quality. These data are input as initial conditions into computational models. For small coupons X-Ray/CT examination is also being performed. In-situ techniques, including acoustic emission, digital image correlation techniques, and non-immersion ultrasonic inspection are also being employed to monitor the onset and propagation of damage, and to provide an indication for test interruption and more detailed examination by X-Ray computed tomography (CT). The following examples illustrate the use of new experimental methods to improve the understanding of the failure processes in composites, to improve the predictive capability of the models, and to validate the models.



### 3.1 Measuring Initial Imperfections with Coordinate Measurement Machine

The response and failure of thin structures subjected to compression loads is strongly affected by small initial imperfections and residual thermal deformations. These initial deformations can be measured using a coordinate measurement machine. This device uses a laser probe to generate high-precision spatial coordinates of millions of points on the surfaces of the specimens. The precision of each point is  $10^{-6}$  mm, which allows an accurate analysis of microscopic deformations. In the photograph shown in Fig. 14, the CMM is used to characterize the deformation of a single stringer compression specimen before it is tested to failure. The measured shape of the skin (Fig. 15a), can be compared to the predicted residual thermal deformation (Fig. 15b). These initial shapes are then incorporated into the analysis model to be used for predicting the nonlinear response of the structure.

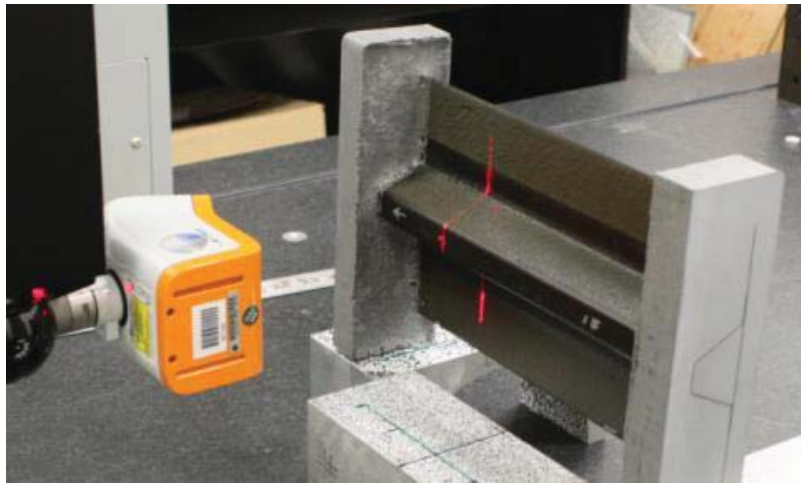
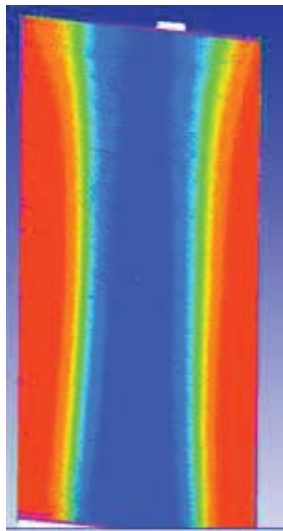
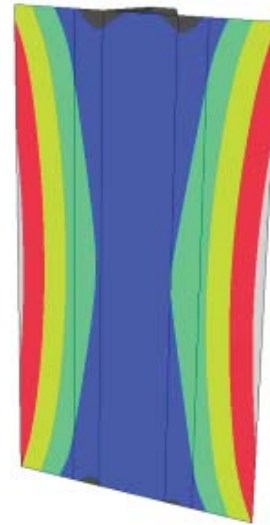


Fig. 14. Measurement of geometric imperfections using the Coordinate Measurement Machine with a laser probe.



(a) Measured imperfection



(b) Predicted residual deformation

Fig. 15. Measured imperfection and predicted residual deformation after thermal cool down.

### 3.2 Ultrasonic Inspection

New non-immersion high-definition ultrasonic measurement (UT) systems are being routinely applied to inspect specimens before tests. The UT system, which is shown below uses a focused immersion probe mounted in a captive water column with a rugged Nitrile membrane tip at the focal point. Performing inspections before the tests ensures that any defects are properly accounted for in data interpretation and in analysis simulations. For instance, it was found during a routine scan of the specimen shown below that an anomaly was present along the stiffener flange (Fig. 16). The specimen was nevertheless tested to failure and its collapse load was significantly lower than expected. Without the initial scan, the manufacturing defect would have gone unnoticed and the results of the test could have been misunderstood.

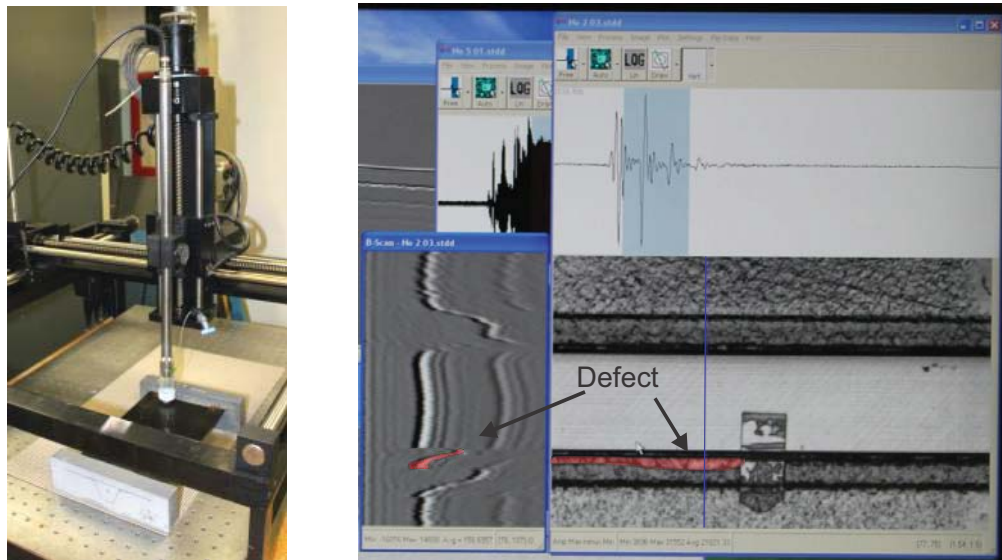


Fig. 16. Pre-test ultrasonic inspection of experimental test articles.

A non-immersion system has also been developed for in-situ application [77] so that damage initiation and progression can be monitored while a specimen is under load (Fig. 17). This capability has been used during the testing of specimens loaded monotonically and for specimens loaded in fatigue until failure. The system uses normal-incidence pulse-echo ultrasound, which is optimal for detecting delaminations, but is not as good for characterizing matrix cracking. Methods employing non-normal incidence ultrasound, or polar backscattering, are being developed to provide a rapid capability for a more complete characterization of damage, including measurement of matrix cracking [78].



Fig. 17. Non-immersion in-situ ultrasound (UT) system.

### 3.3 Digital Image Correlation

Digital image correlation (DIC) is being used during testing to track the onset and growth of surface damage, and to develop methodologies for determining crack growth as a function of load. Methods for determining sub-surface damage from changes in surface strain profiles are also being investigated.

In a recent application, a methodology using the commercial measuring system Vic-3D [79] was developed to characterize the fracture of composite joints bonded with Cytec FM 300-M adhesive [80]. A test campaign was conducted using three types of specimens. Double Cantilever Beam, End Notch Flexure and Mixed-Mode Bending tests were performed on bonded carbon-epoxy specimens to determine the mode I, mode II, and mixed-mode fracture properties, respectively. The characterization procedure uses DIC to extract the displacement histories around the initial crack tip (Fig. 18a-c). Following an inverse methodology, these displacements are substituted into analytical J-integral equations that describe the fracture energy (ERR), Fig. 18d. Finally, the cohesive laws needed for finite element analysis are obtained by numerical differentiation of the J-integral functions. The resulting cohesive laws represent the adhesive stiffness, strength, and fracture resistance in the form of stress-displacement functions in each mode of fracture (Fig. 18).

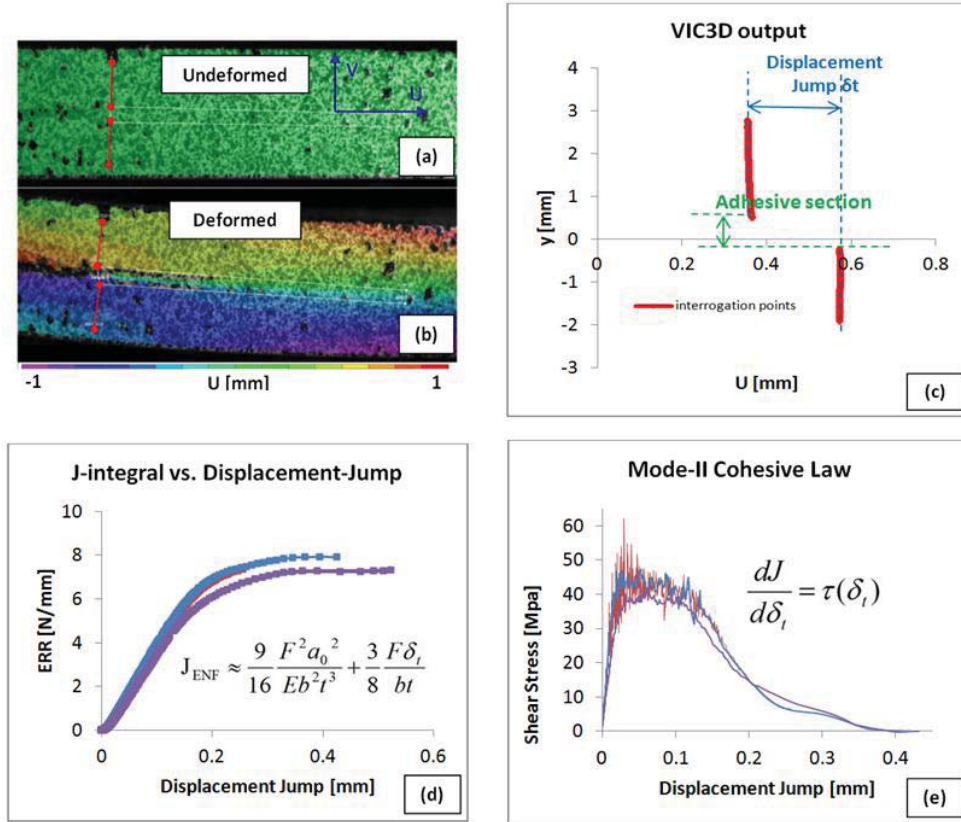


Fig. 18. Procedure to estimate the Mode II cohesive law: (a) displacement field around the crack-tip without external load; (b) displacement field around the crack-tip at maximum load; (c) output from the interrogation of the vertical line through the crack tip; (d) J-integral vs. displacement-jump; and (e) the experimental cohesive law.

### 3.4 X-Ray Computed Tomography

Recent advances in X-Ray/CT capability have provided the opportunity for detailed examination of damage development and evolution in the interior of composite structures. Resolution on the order of 10-20  $\mu\text{m}$  is relatively common with commercially available sources, and can be obtained for specimens of laboratory scale with reasonable data acquisition and reconstruction times. The ability to obtain three-dimensional images of damage patterns provides the data necessary to tremendously increase understanding of the mechanisms of damage development and interaction, and to quantify predictive capability in terms of damage development as well as ultimate load. Additional advances in ultra-high resolution CT ( $\sim 0.5 \mu\text{m}$ ) are yielding images of damage mechanisms with spatial resolutions below the ply thickness [1, 81]. Data at this scale may be required for improving understanding of the mechanisms involved in the initiation and early stages of damage evolution, the interactions of matrix cracks with fiber failures, and may be critical for refinement of fatigue damage models.

X-Ray/CT examination has become a critical component in the validation process of the damage models. Nondestructively imaging internal damage, during interrupted tests, provides the opportunity to monitor progression of damage with load for comparison with the damage predictions. A sample image shown in Fig. 19 obtained from an open-hole tension specimen shows the ability to resolve both delaminations and matrix cracks. Data acquisition and reconstruction times, however limit application of X-Ray/CT examination to small specimens or

very small regions of specimens for ultra-high resolution inspection. New X-Ray sources and significantly reduced data acquisition and reconstruction times are required for in-situ high-resolution inspection and inspection of large parts.

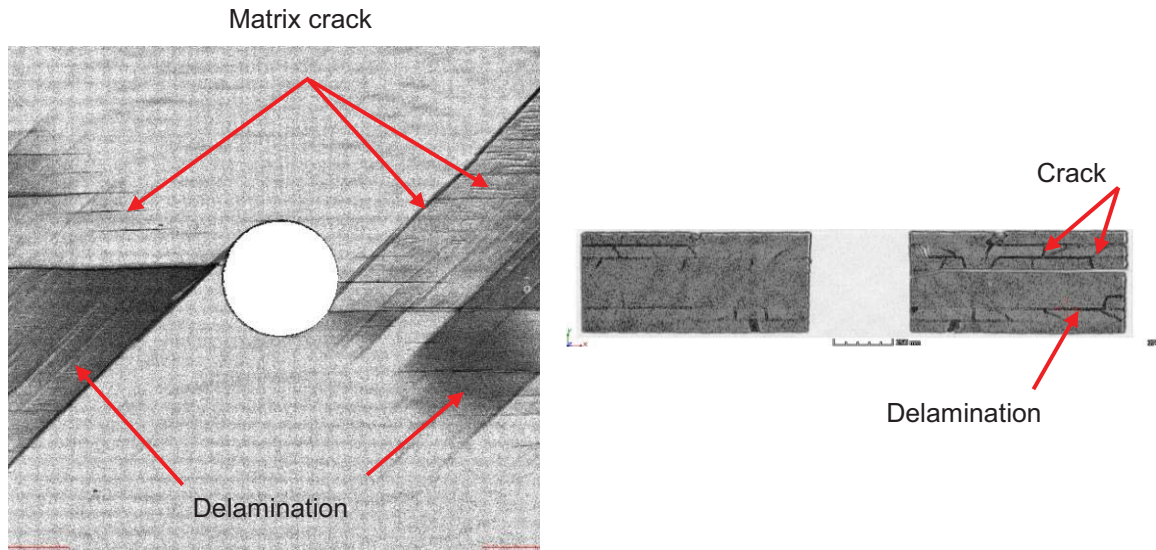


Fig. 19. X-Ray/CT to monitor internal damage development.

### 3.5 Summary, Experimental Methods

**3 Experimental Methods**

**State of the Art**

- *In-situ digital image correlation, ultrasonic inspection (UT) routinely performed for laboratory scale specimens.*
- *X-Ray/CT capability with resolution on the order of 5-20  $\mu\text{m}$ , common with commercially available sources, can resolve matrix cracks and delaminations. Data acquisition and reconstruction times are reasonable for laboratory scale specimens.*

**Recent Advances**

- *The Nondestructive Evaluation Sciences Branch (NESB) and The Structural Mechanics and Concepts Branch (SMCB) at LaRC have spurred the development of in-situ UT inspection capability, and rapid UT inspection capability for large structural sub-components.*
- *Emerging stereo microscope digital image correlation systems provide order of magnitude increase in resolution over conventional lenses, and provide potential ability to detect precursors to crack nucleation.*



- *Emerging ultra-high resolution CT (~0.5  $\mu\text{m}$ ) provides spatial resolution below the ply thickness.*

***Technology Barriers***

- *Data acquisition and reconstruction times limit application of X-Ray/CT examination to small specimens, or very small regions of specimens for ultra-high resolution inspection. New X-ray sources and significantly reduced data acquisition times are required for high resolution in-situ inspection and inspection of large parts.*
- *In-situ ultrasonic inspection is in general limited to characterization of delamination. Developments are required in array-based polar backscattering approaches for characterizing transverse matrix cracks and delaminations.*

## 4 Applications

### 4.1 Damage Tolerance of Post Buckled Stiffened Panels

Rotorcraft fuselages are usually thin, so they are susceptible to buckling at low strain levels. Major gains in structural efficiency can be achieved by exploiting the ability of stiffened composite structures to operate deep into the postbuckling regime. These potential weight savings are not yet fully achievable, mainly because of the difficulty in predicting the strength of composite structures, and the difficulty in determining the durability and damage tolerance of postbuckled structures. Consequently, there is increasing interest in the study of damage tolerant structures. Using the specially-developed Single Stringer Compression Specimen (SSCS) shown in Fig. 20, experimental and analytical studies have been conducted to investigate the effects of bond defects, geometric imperfections, and postbuckling response on the collapse of stiffened composite panels.

Predicting the failure of stiffened panels in postbuckling is difficult for several reasons. One of the difficulties is associated with numerical convergence when the nonlinearities induced by propagating material failures are interacting with geometric non-linearity as a result of the large post-buckling deformations. An additional difficulty is the sensitivity of the panel response to initial geometric imperfections, because the postbuckling response paths and the associated failure modes can differ among nominally identical panels due to the presence of the initial geometric imperfections. A study of the effect of geometric imperfections on the predicted response was conducted by applying small perturbations in the skin normal direction to the locations of the nodes in the finite element model. The maximum perturbation was kept at 1/10 of the skin thickness. The distribution of the perturbations was calculated by linear combinations of the first three buckling modes. It was found from a large number of analyses that different imperfections resulted in one of the three different responses shown in Fig. 21. The differences in the postbuckling responses are particularly important in the presence of defects or pre-existing damage. For instance, a bond defect between skin and stringer at the location shown in Fig. 21 is more likely to propagate if the deformation is of Type A, where the skin pulls away from the stringer, as opposed to Type C, where the deflections of the skin are small, or Type B, where the skin deflects into the stringer.

The collapse of single stringer specimens is sudden, making it difficult to determine the sequence of events that lead to the catastrophic failure. High-speed video recorded during the tests confirms the numerical predictions: the postbuckling deformations cause a local pull-off of the stringer flange from the skin, as shown in Fig. 22. The ensuing delamination grows under the stringer, which becomes unstable and it fails in a crippling mode. The digital image correlation

system records the critical deformations of the skin, which are shown in Fig. 23. A change in the buckling mode of the skin inside the stringer initiates a pull-off (Fig. 23a and Fig. 23b) and results in a detachment of the skin along the entire specimen (Fig. 23c).

## Damage Tolerance of Postbuckled Composite Airframe

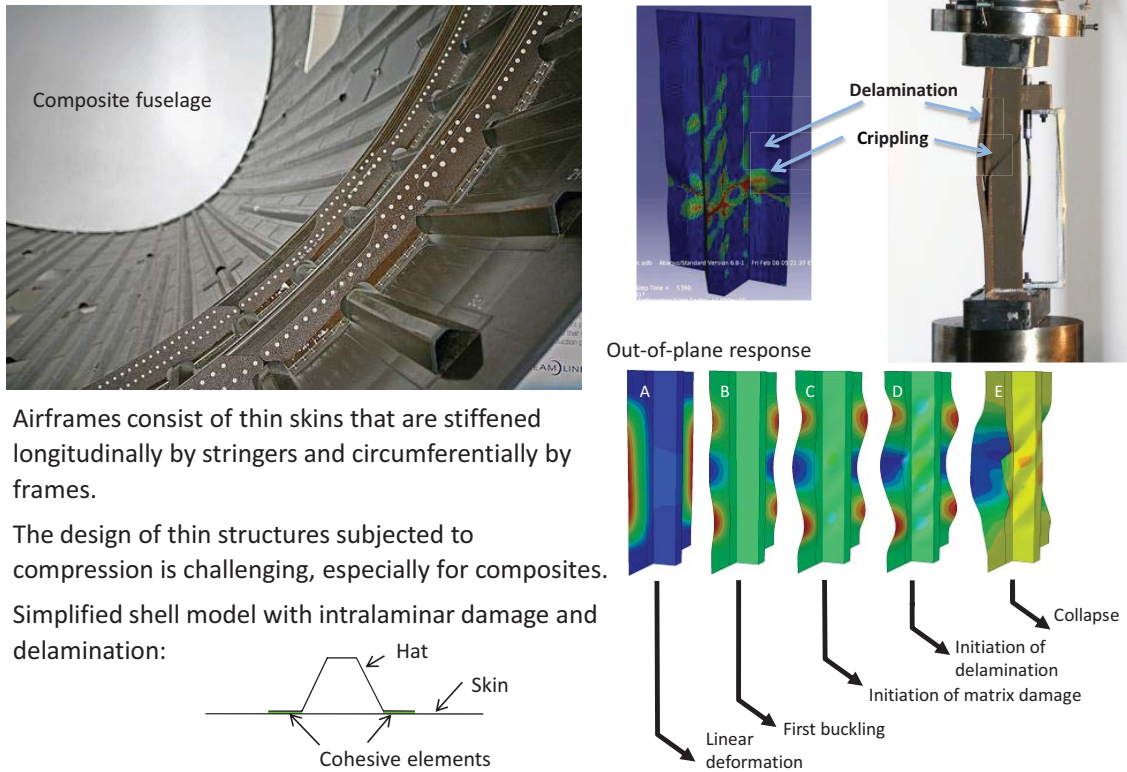


Fig. 20. The Single Stringer Compression Specimen was developed to investigate the damage tolerance of postbuckled stiffened structures.

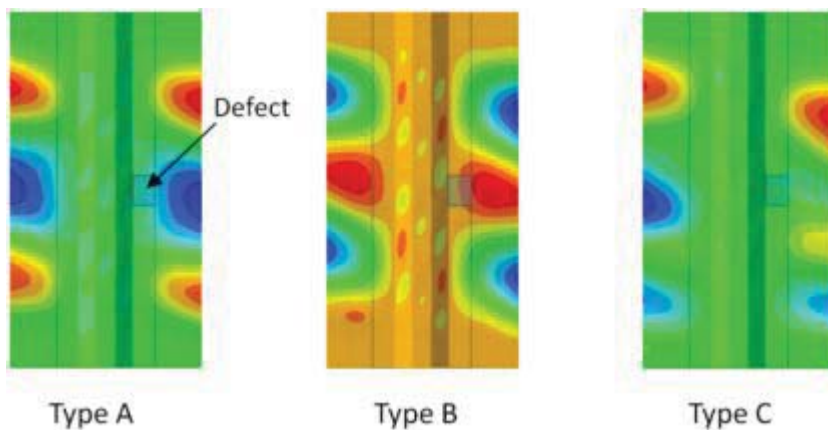


Fig. 21. Three postbuckling response types predicted using different initial geometric imperfections.

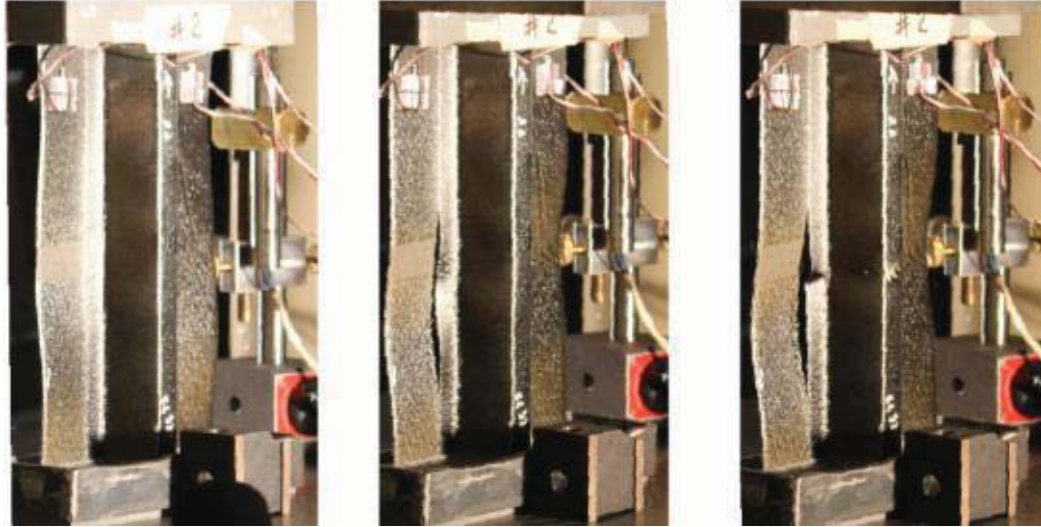


Fig. 22. Failure sequence in SSCS specimen exhibiting Type A postbuckling response.

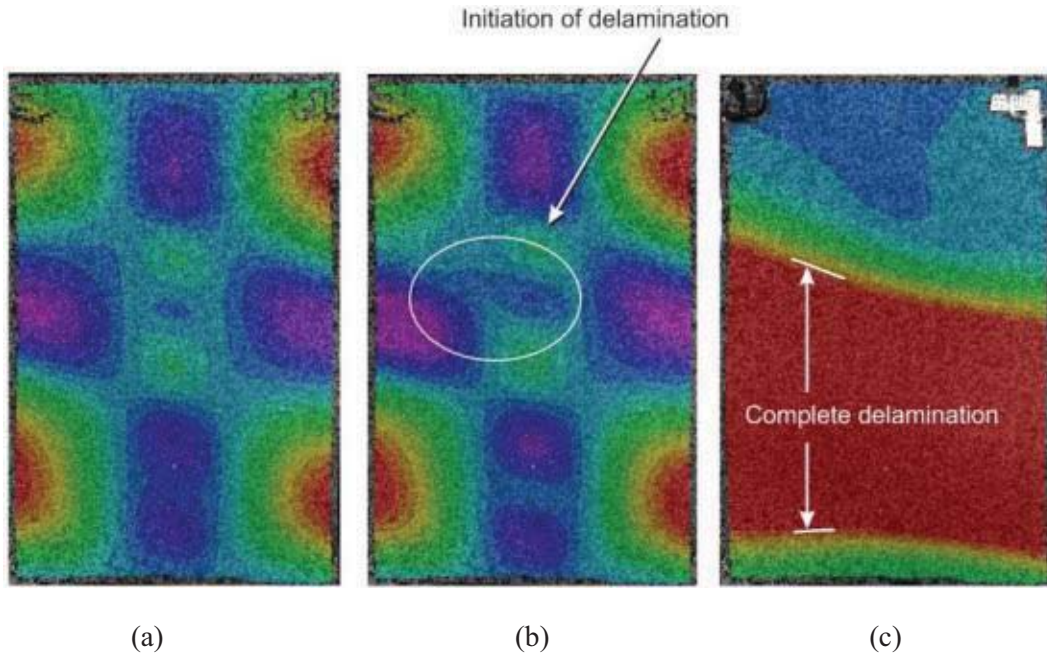


Fig. 23. Type B surface deformation sequence measured using digital image correlation.

## 4.2 Open-Hole Tension

The open-hole tension specimen is one configuration being used to assess the performance of the analysis methods that are being developed. This specimen, although relatively simple in geometry and loading, represents a significant challenge to progressive damage analysis tools, because of the complexity of the damage evolution and interactions that occur prior to ultimate failure. The open-hole tension (OHT) specimen was recently studied, both experimentally and computationally [55, 82]. Specimens were fabricated from IM7/8552 graphite-epoxy and had a quasi-isotropic stacking sequence. Three-dimensional scaling, with ply-level and sub-laminate-



level approaches to through-the-thickness scaling, was examined to determine size effects in laminate failure.

An in-house experimental study is being conducted to examine further the evolution of damage and failure in these specimens, and to assess the modeling approaches that are being developed. Current tests are focused on monotonic tension loading. Specimens have been fabricated for subsequent testing under cyclic loading. Ply-level scaled specimens only are considered in the present study because of the damage modes that develop in these specimens. Ply-level scaled specimens were fabricated by blocking multiple plies with the same orientation together, thereby increasing the effective ply thickness. Two thicknesses are considered with the stacking sequence  $[45_m/90_m/-45_m/0_m]_s$  and with  $m = [2, 4]$ . The plate width to hole diameter ratio,  $w/d$  is kept constant at a value of 5, and the length to hole diameter ratio,  $l/d$ , is equal to 20.

The experimental data indicate that the failure progression and the mode of laminate failure are dependent on the laminate layup (stacking sequence and ply thicknesses) and that the scaling of strength with respect to size is dependent on the type of failure. Sub-critical damage develops at relatively low loads prior to ultimate failure and typically begins with matrix cracks in the off-axis (non-load bearing) plies and progresses through interconnecting delaminations in a complex three-dimensional pattern, as shown in Fig. 24. It is the accumulation of these damage modes that ultimately leads to failure of the specimen. The extent of the sub-critical damage development is dependent on the laminate geometry and significantly influences the laminate failure mode. Three failure modes have been identified, and are classified as brittle, pull-out and delamination failure modes [55]. The brittle failure mode is relatively easy to predict, the remaining are difficult.

The two computational schemes described above, CDM for in-plane damage coupled with interface elements for interlaminar damage, and DDM for in-plane damage coupled with interface elements for interlaminar damage have been employed for predicting the response of the OHT specimens. Complete details of the modeling approaches and analysis predictions can be found in Swindeman [72], and Song *et al.* [58]. The analysis conducted by Swindeman used the Rx-FEM methodology developed by Iarve [71]. The analysis conducted by Song used the standard Abaqus CDM model, and a finite element model with the meshes in each ply aligned with the fiber direction to address the CDM limitations described above. Analyses were also conducted by Song using a radial mesh in all plies to demonstrate the inability to predict the complex damage evolution using traditional modeling approaches.

Overall load versus end-displacement predictions agreed well with experimentally obtained data, and the effects of scaling on failure load were well predicted for the delamination failure mode. In addition, predicted damage patterns qualitatively agree well with experimentally obtained images of damage development. An example comparison of predictions and experimental data for a specimen with a 1/8-inch diameter hole, just prior to specimen failure is provided in Fig. 24. In all figures, delamination damage at the interface indicated is shown, along with transverse matrix cracks in adjacent plies. In the CDM images, gray areas are delaminations, and red lines are cracks. In the DDM predictions, shaded areas are delaminations, and lines are predicted cracks. In the experimental images gray areas are delaminations and black lines are cracks. As shown, both computational methods are able to predict well the complex damage patterns experimentally observed. The CDM predictions show fewer matrix cracks than the DDM predictions, and in the experimentally observed damage. These additional matrix cracks are in some cases significant and can allow for link-up of damage through the thickness of the laminate, earlier than the case with fewer matrix cracks. Additionally matrix cracks in the different plies are loaded in different mixed-mode conditions, and the eventual interaction of the cracks with delaminations and cracks in adjacent layers allows for little error in FE predictions, (e.g., the modeled growth of a crack in one ply may either unduly arrest or promote crack growth in an adjacent ply if not well-predicted). More study is required to determine the significance of the link-up, which is likely to be specimen and loading dependent. It is anticipated that a predicted

delay in link-up will be significant for fatigue loading conditions. Analyses are currently in progress to assess the capabilities of refinements to the in-house continuum damage mechanics (CDM) finite element (FE) subroutine in properly representing these interactions.

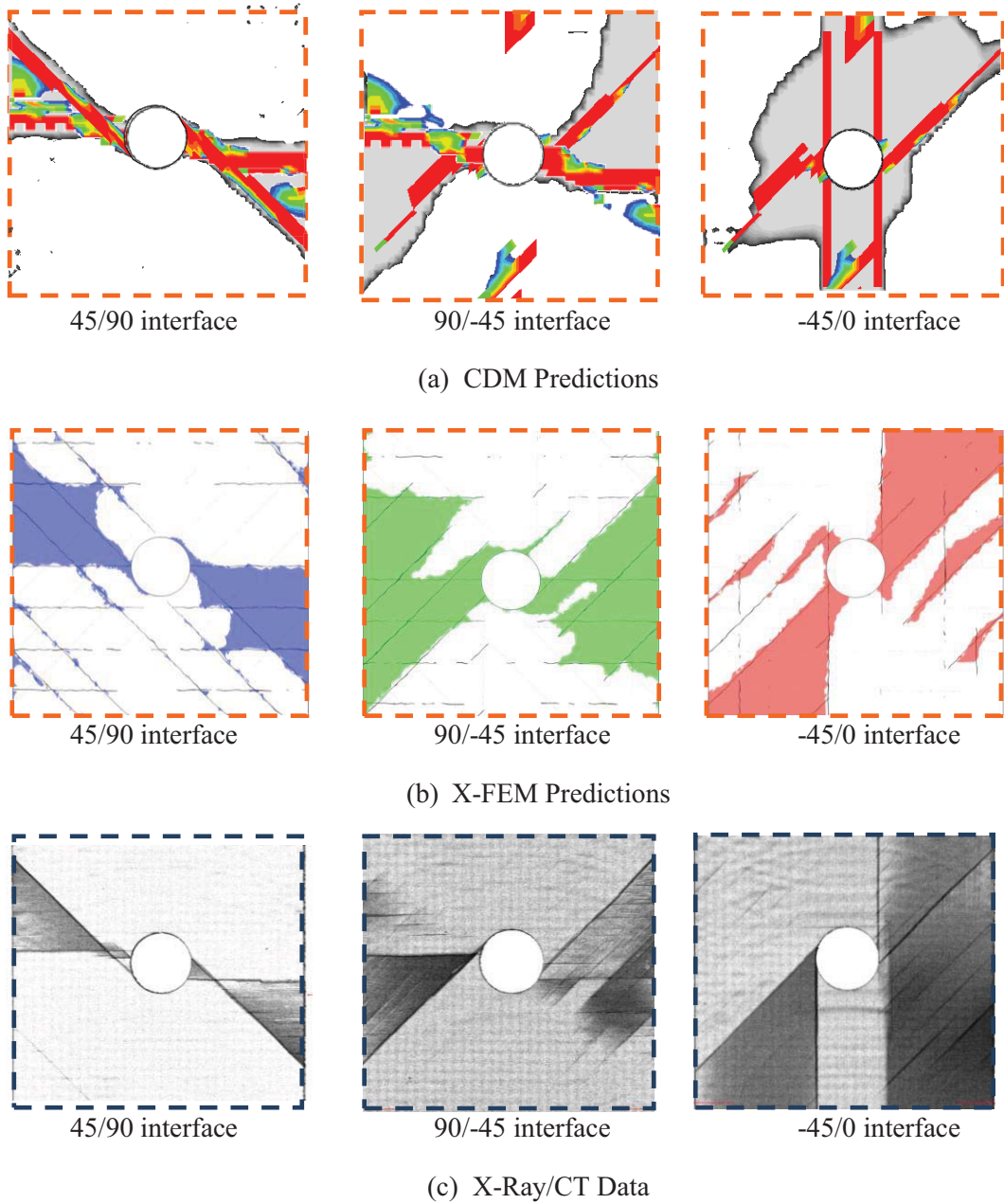


Fig. 24. Comparison of analysis predictions using CDM [59] and X-FEM [14] models with X-Ray/CT data at a point just beyond peak load for  $[45_4/90_4/-45_4/0_4]_s$  specimens with a 1/8-inch diameter hole.

Finally, experimental methods and data reduction methods are being developed to quantify crack densities and lengths at various load levels, to obtain crack initiation data, and to obtain crack-length versus load data. Crack initiation data for subsurface plies is being obtained, within the limits of current resolution, using acoustic emission coupled with X-Ray/CT. Crack initiation and crack growth data for surface plies are being obtained using digital image correlation. These

data will be used to aid in the calibration of the cohesive laws used in the analysis predictions, and to aid in the critical assessment of the analysis models.

## 5 Summary

Damage models for composites have quickly been increasing in diversity and complexity, and continuous technological breakthroughs are improving their predictive capabilities. Essential contributions to the development of numerous new modeling capabilities and to the formulation of the conditions under which given models can be expected to work have recently been made. An overview of recent developments in damage modeling for laminated composites was presented with the goal of defining the state of the art, the immediate technological barriers and for outlining potential solutions for research. In particular, the capabilities of advanced continuum damage mechanics models, cohesive zone models, and X-FEM models were reviewed and their pathological deficiencies were discussed. Issues of objectivity of the fracture propagation with the various models were discussed and the application of the methods was illustrated with examples of structural analysis. Finally, advances in experimental methods that are necessary for understanding the damage mechanisms in composites and for developing and validating the models were discussed. Non-destructive evaluation methods such as non-immersion UT scanners, digital image correlation, and X-Ray CT are providing rich experimental information on the response and failure of composite materials that is necessary for the development and validation of the computational models.

## References

1. Wright P, Moffat A, Sinclair I, Spearing SM (2010) High Resolution Tomographic Imaging and Modelling of Notch Tip Damage in a Laminated Composite. *Compos Sci Technol.* **70**.(10): 1444-1452.
2. Mollenhauer D, Ward L, Iarve E, et al. (2012) Simulation of Discrete Damage in Composite Overheight Compact Tension Specimens. *Comp A.* **43**.(10): 1667-1679.
3. van der Meer FP, Oliver C, Sluys LJ (2010) Computational Analysis of Progressive Failure in a Notched Laminate Including Shear Nonlinearity and Fiber Failure. *Compos Sci Technol.* **70**.(4): 692-700.
4. Fang XJ, Zhou ZQ, Cox BN, Yang QD (2011) High-Fidelity Simulations of Multiple Fracture Processes in a Laminated Composite in Tension. *J Mech Phys Solids.* **59**.(7): 1355-1373.
5. González C, Llorca J (2007) Mechanical Behavior of Unidirectional Fiber-Reinforced Polymers under Transverse Compression: Microscopic Mechanisms and Modeling. *Compos Sci Technol.* **67**.(13): 2795-2806.
6. Maimí P, Camanho PP, Mayugo JA, Dávila CG (2007) A Continuum Damage Model for Composite Laminates: Part I - Constitutive Model. *Mech Mater.* **39**.(10): 897-908.
7. Camanho PP, Dávila CG, de Moura MFSF (2003) Numerical Simulation of Mixed-Mode Progressive Delamination in Composite Materials. *J Compos Mater.* **37**.(16): 1415-1438.
8. Krueger R (2002) The Virtual Crack Closure Technique: History, Approach and Applications. *NASA/CR-2002-211628.*, Hampton, VA.
9. Mabson G, Lyle RD, Dopker B, Hoyt DM, Baylor JS, Graesser DL (2007) Fracture Interface Elements for Static and Fatigue Analysis. Proc *16th International Conference on Composite Materials*, Kyoto, Japan.
10. van der Meer FP, Sluys LJ (2009) Continuum Models for the Analysis of Progressive Failure in Composite Laminates. *J Compos Mater.* **43**.(20): 2131-2156.

11. Iarve EV, Mollenhauer D, Kim R (2005) Theoretical and Experimental Investigation of Stress Redistribution in Open Hole Composite Laminates Due to Damage Accumulation. *Comp A*. **36**(2): 163-171.
12. CMH-17 (2011) Materials Usage, Design and Analysis, Vol. 2, Rev G. *Composite Materials Handbook*. SAE, Philadelphia, PA.
13. van der Meer FP, Sluys B, Hallett SR, Wisnom M (2012) Computational Modeling of Complex Failure Mechanisms in Laminates. *J Compos Mater*. **46**(5): 603-623.
14. Swindeman MJ, Iarve EV, Brockman RA, Mollenhauer DH, Hallett SR (2011) Strength Prediction in Open Hole Composite Laminates by Using Discrete Damage Modeling. *52nd AIAA/ASME/ASCE/AHS/ASC Structures, Structural Dynamics and Materials Conference*, Denver, CO.
15. Griffith AA (1921) The Phenomena of Rupture and Flow in Solids. *Phil Trans Roy Soc of London*. **A 221**. 163-197.
16. Dávila CG, Rose CA, Camanho PP (2009) A Procedure for Superposing Linear Cohesive Laws to Represent Multiple Damage Mechanisms in the Fracture of Composites. *Int J Fracture*. **158**(2): 211-223.
17. Spearing SM, Beaumont PWR, Ashby MF (1992) Fatigue Damage Mechanics of Composite Materials. II: A Damage Growth Model. *Compos Sci Technol*. **44**(2): 169-177.
18. ASTM D5528-01 (2002) Standard Test Method for Mode I Interlaminar Fracture Toughness of Unidirectional Fiber-Reinforced Polymer Matrix Composites. *Annual Book of Astm Standards*. American Society for Testing and Materials, West Conshohocken, PA.
19. Tamuzs V, Tarasovs S, Vilks U (2001) Progressive Delamination and Fiber Bridging Modeling in Double Cantilever Beam Composite Specimens. *Eng Fract Mech*. **68**(5): 513-525.
20. Gutkin R, Laffan ML, Pinho ST, Robinson P, Curtis PT (2011) Modelling the R-Curve Effect and Its Specimen-Dependence. *Int J Solids Structures*. **48**(11-12): 1767-1777.
21. Sorensen L, Botsis J, Gmür T, Humbert L (2008) Bridging Traction in Mode I Delamination: Measurements and Simulations. *Compos Sci Technol*. **68**(12): 2350-2358.
22. Hansen AL, Lund E, Sørensen BF (2007) Simulation of Delamination Including Fiber Bridging Using Cohesive Zone Models. *Proc ECCOMAS Thematic Conference on Mechanical Response of Composites* P.P. Camanho et al., Porto, Portugal.
23. Airoidi A, Dávila CG (2012) Identification of Material Parameters for Modelling Delamination in the Presence of Fibre Bridging. *Compos Struct*. **94**(11): 3240-3249.
24. Högberg JL, Sørensen BF, Stigh U (2007) Constitutive Behaviour of Mixed Mode Loaded Adhesive Layer. *Int J Solids Structures*. **44**(25-26): 8335-8354.
25. Turon A, Camanho PP, Costa J, Renart J (2010) Accurate Simulation of Delamination Growth under Mixed-Mode Loading Using Cohesive Elements: Definition of Interlaminar Strengths and Elastic Stiffness. *Compos Struct*. **92**(8): 1857-1864.
26. Sarrado C, Turon A, Renart J, Urresti I (2012) Assessment of Energy Dissipation During Mixed-Mode Delamination Growth Using Cohesive Zone Models. *Comp A*. **43**(11): 2128-2136.
27. Leone AF, Girolamo D, Dávila CG (2012) Progressive Damage Analysis of Bonded Composite Joints. *NASA/TM-2012-217790*, Hampton.
28. Turon A, Costa J, Camanho PP, Dávila CG (2007) Simulation of Delamination in Composites under High-Cycle Fatigue. *Comp A*. **38**(11): 2270-2282.
29. Turon A, Camanho PP, Costa J, Dávila CG (2006) A Damage Model for the Simulation of Delamination in Advanced Composites under Variable-Mode Loading. *Mech Mater*. **38**(11): 1072-1089.



30. Dávila CG, Camanho PP, Turon A (2008) Effective Simulation of Delamination in Aeronautical Structures Using Shells and Cohesive Elements. *J Aircraft*. **45**.(2): 663-672.
31. Ladevèze P, LeDantec E (1992) Damage Modelling of the Elementary Ply for Laminated Composites. *Compos Sci Technol*. **43**.(3): 257-267.
32. Matzenmiller A, Lubliner J, Taylor RL (1995) A Constitutive Model for Anisotropic Damage in Fiber-Composites. *Mech Mater*. **20**.(2): 125-152.
33. Kachanov LM (1986) *Introduction to Continuum Damage Mechanics*. Martinus Nijhoff, Dordrech, NL.
34. Lemaitre J, Desmorat R, Sauzay M (2000) Anisotropic Damage Law of Evolution. *Euro J Mech A*. **19**.(2): 187-208.
35. Dassault Systèmes (2011) *Abaqus® 6.11 Documentation*. Simulia Corp., Providence, RI, USA.
36. Maimí P, Camanho PP, Mayugo JA, Dávila CG (2006) A Thermodynamically Consistent Damage Model for Advanced Composites. *NASA-TM-2006-214282*, Hampton, VA.
37. Soden PD, Hinton MJ, Kaddour AS (1998) A Comparison of the Predictive Capabilities of Current Failure Theories for Composite Laminates. *Compos Sci Technol*. **58**.(7): 1225-1254.
38. Hinton MJ, Kaddour AS, Soden PD (2002) A Comparison of the Predictive Capabilities of Current Failure Theories for Composite Laminates, Judged against Experimental Evidence. *Compos Sci Technol*. **62**.(12-13): 1725-1797.
39. Dávila CG, Camanho PP, Rose CA (2005) Failure Criteria for Frp Laminates. *J Compos Mater*. **39**.(4): 323-345.
40. Pinho ST, Dávila CG, Camanho PP, Iannucci L, Robinson P (2005) Failure Models and Criteria for Frp under in-Plane or Three-Dimensional Stress States Including Shear Non-Linearity. *NASA/TM-2005-213530*, Hampton, VA.
41. de Borst R (2008) Challenges in Computational Materials Science: Multiple Scales, Multi-Physics and Evolving Discontinuities. *Comput Mater Sci*. **43**.(1): 1-15.
42. Bažant ZP, Oh B (1983) Crack Band Theory for Fracture of Concrete. *Mater Struct*. **16**.(3): 155-177.
43. Maimí P, Camanho PP, Mayugo JA, Dávila CG (2007) A Continuum Damage Model for Composite Laminates: Part II - Computational Implementation. *Mech Mater*. **39**.(10): 909-919.
44. Hansen P, Martin R (1999) DCB, 4ENF and MMB Delamination Characterisation of S2/8552 and IM7/8552. *N68171-98-M-5177*. United States Army European Research Office of the US Army, London, England.
45. Czabaj MW, Ratcliffe JG (2012) Comparison of Intralaminar and Interlaminar Mode-I Fracture Toughness of Unidirectional IM7/8552 Graphite/Epoxy Composite. *Proc American Society for Composites 27th Technical Conference*, Arlington, TX.
46. Pinho ST, Robinson P, Iannucci L (2006) Fracture Toughness of the Tensile and Compressive Fibre Failure Modes in Laminated Composites. *Compos Sci Technol*. **66**.(13): 2069-2079.
47. Catalanotti G, Camanho PP, Xavier JC, Dávila CG, Marques AT (2010) Measurement of Resistance Curves in the Longitudinal Failure of Composites Using Digital Image Correlation. *Compos Sci Technol*. **70**.(13): 1986-1993.
48. Parvizi A, Garrett K, Bailey J (1978) Constrained Cracking in Glass Fibre-Reinforced Epoxy Cross-Ply Laminates. *J Mat Sci*. **13**. 195-201.
49. Wang ASD (1984) Fracture Mechanics of Sublaminar Cracks in Composite Materials. *Comp Tech Rev*. **6**.(2): 45-62.

50. Camanho PP, Dávila CG, Pinho ST, Iannucci L, Robinson P (2006) Prediction of in Situ Strengths and Matrix Cracking in Composites under Transverse Tension and in-Plane Shear. *Comp A*. **37**.(2): 165-176.
51. Hahn HT, Tsai SW (1973) Nonlinear Elastic Behavior of Unidirectional Composite Laminae. *J Compos Mater*. **7**.(1): 102-118.
52. Schuecker C, Dávila CG, Pettermann HE (2008) Modeling the Non-Linear Response of Fiber-Reinforced Laminates Using a Combined Damage/Plasticity Model. *NASA/TM-2008-215314*, Hampton, VA.
53. Ramberg W, Osgood WR (1943) Description of Stress-Strain Curves by Three Parameters. *NACA-TN-902*, Hampton.
54. Sih S, Kim RY, Kawabe K, Tsai SW (2007) Experimental Studies of Thin-Ply Laminated Composites. *Compos Sci Technol*. **67**.(6): 996-1008.
55. Green BG, Wisnom MR, Hallett SR (2007) An Experimental Investigation into the Tensile Strength Scaling of Notched Composites. *Comp A*. **38**.(3): 867-878.
56. Jirásek M (1998) Nonlocal Models for Damage and Fracture: Comparison of Approaches. *Int J Solids Structures*. **35**.(31-32): 4133-4145.
57. Laš V, Zemčík R (2008) Progressive Damage of Unidirectional Composite Panels. *J Compos Mater*. **42**.(1): 25-44.
58. Song K, Li Y, Rose CA (2011) Continuum Damage Mechanics Models for the Analysis of Progressive Failure in Open-Hole Tension Laminates. *52nd AIAA/ASME/ASCE/AHS/ASC Structures, Structural Dynamics and Materials Conference*, Denver, CO.
59. Leone F, Dávila CG (2011) Application of Mixed-Mode Cohesive Damage Laws to Continuum Damage Mechanics. In: Ferreira A (ed) *Proc ICCS16 -16th International Conference on Composite Structures*, Porto, Portugal.
60. Camanho PP, Bessa MA, Catalanotti G, Vogler M, Rolfes R (2012) Modeling the Inelastic Deformation and Fracture of Polymer Composites - Part II: Smearred Crack Model. *Mechanics of Materials*.
61. Moës N, Dolbow J, Belytschko T (1999) A Finite Element Method for Crack Growth without Remeshing. *Int J Num Meth Eng*. **46**.(1): 131-150.
62. Belytschko T, Parimi C, Moës N, Sukumar N, Usui S (2003) Structured Extended Finite Element Methods for Solids Defined by Implicit Surfaces. *Int J Num Meth Eng*. **56**.(4): 609-635.
63. Rudraraju S, Salvi A, Garikipati K, Waas AM (2012) Predictions of Crack Propagation Using a Variational Multiscale Approach and Its Application to Fracture in Laminated Fiber Reinforced Composites. *Compos Struct*. **94**.(11): 3336-3346.
64. Huynh DBP, Belytschko T (2009) The Extended Finite Element Method for Fracture in Composite Materials. *Int J Num Meth Eng*. **77**.(2): 214-239.
65. van der Meer F, Sluys L (2009) A Phantom Node Formulation with Mixed Mode Cohesive Law for Splitting in Laminates. *Int J Fracture*. **158**.(2): 107-124.
66. Ling D, Yang Q, Cox B (2009) An Augmented Finite Element Method for Modeling Arbitrary Discontinuities in Composite Materials. *Int J Fracture*. **156**.(1): 53-73.
67. Iarve EV (2003) Mesh Independent Modelling of Cracks by Using Higher Order Shape Functions. *Int J Num Meth Eng*. **56**.(6): 869-882.
68. Patzák B, Jirásek M (2003) Process Zone Resolution by Extended Finite Elements. *Eng Fract Mech*. **70**.(7-8): 957-977.
69. Benvenuti E (2008) A Regularized Xfem Framework for Embedded Cohesive Interfaces. *Comp meth Appl Mech Eng*. **197**.(49-50): 4367-4378.



70. Oliver J, Huespe AE, Sánchez PJ (2006) A Comparative Study on Finite Elements for Capturing Strong Discontinuities: E-Fem Vs X-Fem. *Comp meth Appl Mech Eng.* **195**.(37-40): 4732-4752.
71. Iarve EV, Gurvich MR, Mollenhauer DH, Rose CA, Dávila CG (2011) Mesh-Independent Matrix Cracking and Delamination Modeling in Laminated Composites. *Int J Num Meth Eng.* **88**.(8): 749-773.
72. Swindeman MJ (2011), "A Regularized Extended Finite Element Method for Modeling the Coupled Cracking and Delamination of Composite Materials," Doctor of Philosophy in Mechanical Engineering, The School of Engineering, University of Dayton, Dayton, OH.
73. Li X, Hallett SR, Wisnom MR, Zobeiry N, Vaziri R, Poursartip A (2009) Experimental Study of Damage Propagation in over-Height Compact Tension Tests. *Comp A.* **40**.(12): 1891-1899.
74. Fang XJ, Yang QD, Cox BN, Zhou ZQ (2011) An Augmented Cohesive Zone Element for Arbitrary Crack Coalescence and Bifurcation in Heterogeneous Materials. *Int J Num Meth Eng.* **88**.(9): 841-861.
75. van der Meer FP, Sluys LJ (2010) Mesh-Independent Modeling of Both Distributed and Discrete Matrix Cracking in Interaction with Delamination in Composites. *Eng Fract Mech.* **77**.(4): 719-735.
76. van der Meer FP, Dávila CG (2013) Cohesive Modeling of Transverse Cracking in Laminates under in-Plane Loading with a Single Layer of Elements Per Ply. *Int J Solids Structures.* **50**.(20–21): 3308-3318.
77. Seebo J, Johnston P (2010) High Speed Position Synchronized Data Acquisition System for in-Situ Ultrasonic Inspection. *Proc 2010 ASNT Spring Conference, Williamsburg, VA.*
78. Johnston PH, Appleget CD, Odarczenko MT (2013) Characterization of Delaminations and Transverse Matrix Cracks in Composite Laminates Using Multiple-Angle Ultrasonic Inspection. *Proc AIP Conference Proceedings*, 1011.
79. Correlated Solutions (2012) *VIC-3D User Manual*, Columbia, SC.
80. Leone FA, Girolamo D, Dávila CG (2012) Progressive Damage Analysis of Bonded Composite Joints. *NASA/TM-2012-217790*, Hampton, VA.
81. Scott AE, Mavrogordato M, Wright P, Sinclair I, Spearing SM (2011) In Situ Fibre Fracture Measurement in Carbon-Epoxy Laminates Using High Resolution Computed Tomography. *Compos Sci Technol.* **71**.(12): 1471-1477.
82. Hallett SR, Green BG, Jiang WG, Wisnom MR (2009) An Experimental and Numerical Investigation into the Damage Mechanisms in Notched Composites. *Comp A.* **40**.(5): 613-624.

**REPORT DOCUMENTATION PAGE**

*Form Approved  
OMB No. 0704-0188*

The public reporting burden for this collection of information is estimated to average 1 hour per response, including the time for reviewing instructions, searching existing data sources, gathering and maintaining the data needed, and completing and reviewing the collection of information. Send comments regarding this burden estimate or any other aspect of this collection of information, including suggestions for reducing this burden, to Department of Defense, Washington Headquarters Services, Directorate for Information Operations and Reports (0704-0188), 1215 Jefferson Davis Highway, Suite 1204, Arlington, VA 22202-4302. Respondents should be aware that notwithstanding any other provision of law, no person shall be subject to any penalty for failing to comply with a collection of information if it does not display a currently valid OMB control number.  
**PLEASE DO NOT RETURN YOUR FORM TO THE ABOVE ADDRESS.**

<b>1. REPORT DATE (DD-MM-YYYY)</b> 01-07-2013		<b>2. REPORT TYPE</b> Technical Memorandum		<b>3. DATES COVERED (From - To)</b>	
<b>4. TITLE AND SUBTITLE</b>  Analysis Methods for Progressive Damage of Composite Structures				<b>5a. CONTRACT NUMBER</b>	
				<b>5b. GRANT NUMBER</b>	
				<b>5c. PROGRAM ELEMENT NUMBER</b>	
<b>6. AUTHOR(S)</b>  Rose, Cheryl A.; Davila, Carlos G.; Leone, Frank A.				<b>5d. PROJECT NUMBER</b>	
				<b>5e. TASK NUMBER</b>	
				<b>5f. WORK UNIT NUMBER</b>  794072.02.07.03.03	
<b>7. PERFORMING ORGANIZATION NAME(S) AND ADDRESS(ES)</b> NASA Langley Research Center Hampton, VA 23681-2199				<b>8. PERFORMING ORGANIZATION REPORT NUMBER</b>  L-20257	
<b>9. SPONSORING/MONITORING AGENCY NAME(S) AND ADDRESS(ES)</b> National Aeronautics and Space Administration Washington, DC 20546-0001				<b>10. SPONSOR/MONITOR'S ACRONYM(S)</b>  NASA	
				<b>11. SPONSOR/MONITOR'S REPORT NUMBER(S)</b>  NASA/TM-2013-218024	
<b>12. DISTRIBUTION/AVAILABILITY STATEMENT</b> Unclassified - Unlimited Subject Category 24 Availability: NASA CASI (443) 757-5802					
<b>13. SUPPLEMENTARY NOTES</b>					
<b>14. ABSTRACT</b>  This document provides an overview of recent accomplishments and lessons learned in the development of general progressive damage analysis methods for predicting the residual strength and life of composite structures. These developments are described within their State-of-the-Art (SoA) context and the associated technology barriers. The emphasis of the authors is on developing these analysis tools for application at the structural level. Hence, modeling of damage progression is undertaken at the mesoscale, where the plies of a laminate are represented as a homogenous orthotropic continuum. The aim of the present effort is establish the ranges of validity of available models, to identify technology barriers, and to establish the foundations of the future investigation efforts. Such are the necessary steps towards accurate and robust simulations that can replace some of the expensive and time-consuming "building block" tests that are currently required for the design and certification of aerospace structures.					
<b>15. SUBJECT TERMS</b>  Composites; Damage models; Material characterization; Nondestructive evaluation					
<b>16. SECURITY CLASSIFICATION OF:</b>			<b>17. LIMITATION OF ABSTRACT</b>	<b>18. NUMBER OF PAGES</b>	<b>19a. NAME OF RESPONSIBLE PERSON</b>
<b>a. REPORT</b>	<b>b. ABSTRACT</b>	<b>c. THIS PAGE</b>			STI Help Desk (email: help@sti.nasa.gov)
U	U	U	UU	48	<b>19b. TELEPHONE NUMBER (Include area code)</b>  (443) 757-5802